JAERI-M
6848

FILM BOILING HEAT TRANSFER DURING REFLOOD PROCESS

December 1976

Yukio SUDO and Yoshio MURAO

日本原子力研究所
Japan Atomic Energy Research Institute

JAERI-M 6848

Film Boiling Heat Transfer during Reflood Process

Yukio SUDO and Yoshio MURAO

Division of Reactor Safety, Tokai, JAERI

(Received December 1, 1976)

From Westinghouse's Full Length Emergency Cooling Heat Transfer (FLECHT) test data and the previous studies on the film boiling, local subcooling is found to be a dominant factor in the film boiling heat transfer, existing in the reflood process.

By experiment, the correlation was obtained between saturated film boiling heat transfer coefficient h_c,sat and subcooled h_c, sub. The h_c, sat is similar to Bromley's expression, but the value differs from his. The ratio of h_c, sub to h_c, sat is expressed with the local coolant subcooling T_{sub} (°C) as

$$h_c, \text{ sub}/h_c, \text{ sat} = 1 + 0.025\ \Delta T_{sub} .$$

The results in experiment are predicted by this formula with error ± 20% .

JAERI－M 6848

再冠水時の膜沸騰熱伝達の研究

日本原子力研究所東海研究所安全工学部
数土幸夫・村尾良夫

（1976年12月1日受理）

再冠水時に出現する流動伝熱現象の一部を形成している膜沸騰熱伝達について，米国のPWR－FLECHT実験結果の検討とこれまでの膜沸騰に関する理論解析・実験の検討，並びにモデル実験結果の考察から，その支配的要因を明らかにした。

その結果，入口サブクール度，供給流速，発熱量の効果は局所の冷却材のサブクール度として膜沸騰熱伝達に影響を与え，このサブクール度が膜沸騰熱伝達特性に大きな影響を与えていることが明らかとなった。

サブクール度を有する時の膜沸騰熱伝達率 $h_{c,sub}$ は，Bromleyが提唱した飽和膜沸騰熱伝達率の表式を修正した $h_{c,sat}$ と局所のサブクール度 $\triangle T_{sub}$ とで次の関係で表わすことができる。

$$h_{c,sub} = (1+0.025 \cdot \triangle T_{sub}) \cdot h_{c,sat}$$

上式の誤差は±20%以内である。

Contents

List of Table and Figures

1. Introduction

1.1 Reflood Phenomena

On the evaluation of the light water reactor safety, the loss-of-coolant accident is considered to be severe as one of postulated accident.

In this accident, the coolant would be evaluated from the break point of the primary loop and the temperature of the core would be resulted to increase because of low cooling capacity.

To avoid the failure of the core due to excessive temperature rise, the low pressure coolant injection system (LPCIS), which is one of emergency core cooling system (ECCS), is actuated to inject water into the reactor primary loop to flood and cool the core.

When the hot core is flooded with the water of LPCI, various kinds of heat transfer mode and interesting flow patterns are observed. Such a process is called "reflood process". As for the heat transfer modes, for example, convection, nucleate boiling, film boiling and two-phase flow cooling of steam and droplets are co-existing in coolant channels.

1.2 Objective of the Study

In the various heat transfer modes during reflood process, we intended to make clear the characteristics of film boiling heat transfer region in order to provide the information for the computor coding of safety analysis. The objective of the study is to determine the dominant physical factors on the film boiling heat transfer region by using the FLECHT test data[1] which will be described in latter section and to evaluate quantitatively the heat transfer coefficients by using the data of our model experiment and the FLECHT test.

In this sutdy it was attempted, as a first step, to evaluate the influences of the dominant physical factors especially on the film boiling heat transfer region by using the FLECHT test data and second, to evaluate the heat transfer coefficients.

1.3 Review of PWR FLECHT Test

The PWR FLECHT test data which is first analyzed in this report, is

summarized in WCAP-7435[1]. The geometry of the test bundle was chosen to represent a typical pressurized water reactor fuel assembly. Principal dimensions are as follows.

(1) Rod bundle array - 7×7 and 10×10 rods (Square array)

(2) Heater rod length and diameter - 12 feet in heated length and 0.422 inches in diameter

(3) Indirect heating rods

(4) Heater rod pitch - 0.563 inches in square pitch

The axial and radial power distribution are employed to correspond to those that would be found in commercial PWR fuel assemblies. The axial distribution used in FLECHT test is illustrated in Fig. 1 and the power is changed with time following the decay heat curve (refer to Fig.2). The conditions of 36 runs, which was analyzed in this report with regard to the film boiling region, are summarized in Table 1. The parameters of run conditions are bundle size, pressure, power, injected water velocity and inlet water subcooling and the initial heater rod temperature. These runs are characterized with the injected water velocity constant during each run.

1.4 Nomenclature

a_v ; vapour film thickness
a, b, c, Co; constant factor
C_p ; specific heat of vapour at constant pressure
C_{pL}; specific heat of water
D, d; diameter of tube or heater rod
g_c ; gravitational acceleration
h ; heat transfer coefficients
h_c ; convective heat transfer coefficients
h_r ; radiative heat transfer coefficients
h_t ; total heat transfer coefficients
h_{fg}; latent heat of water
k_L ; thermal conductivity of water
k_s ; thermal conductivity of flow tube wall
k_v ; thermal conductivity of steam
L ; representative length of film boiling
ℓ ; elevation of heater rod

P ; pressure

Q, q; heat flux

R ; radius of heater rod

r ; axial distance (variable)

T_G ; gas temperature

T_{in}; Inlet water temperature

$\bar{T}_G$; average gas temperature

T_L ; water temperature

T_Q ; Quench temperature

T_s ; saturation temperature

T_v ; vapour temperature

T_w ; heater rod surface temperature

t ; time

U_{in}; inlet water velocity

U_q ; quench velocity

U_o ; inlet water velocity

V ; water velocity

Z ; distance along the heater rod (variable)

ΔT_{sub}; subcooling

γ ; specific weight

δ ; wall thickness

ε ; emissivity

σ ; Boltzmann's constant, surface tension

ρ ; density

λ_c ; critical length

μ_v ; viscosity

η ; power distribution ratio

ξ ; decay heat power ratio

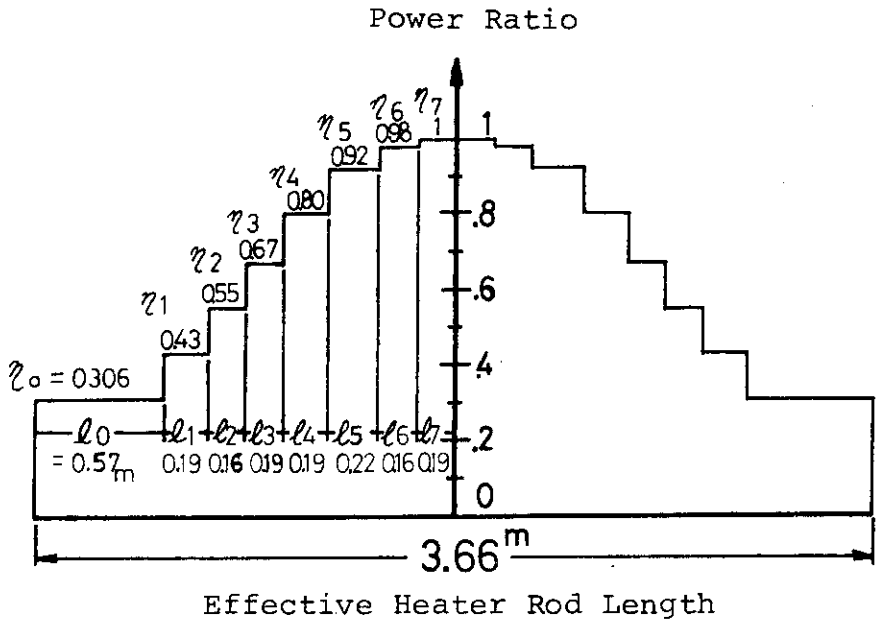

Fig.1 Power Ratio Profile along the Heater Rod in PWR FLECHT Test

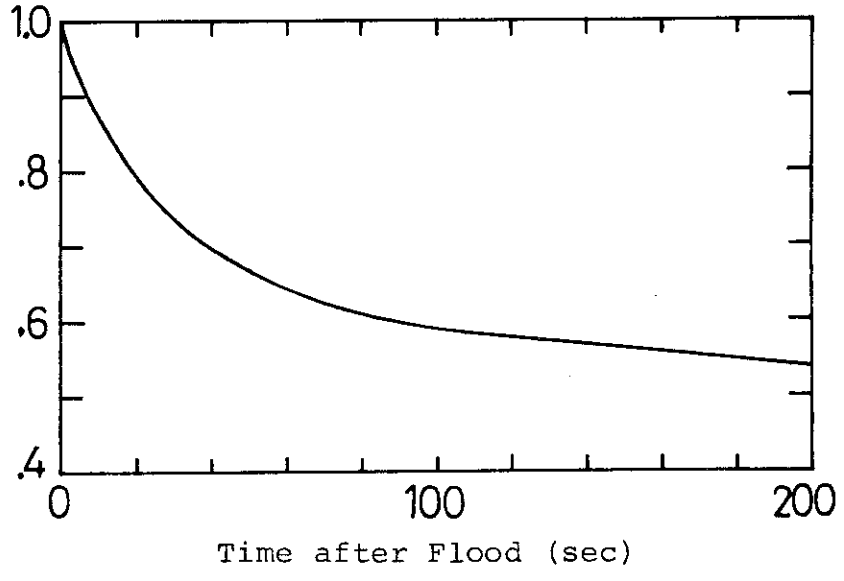

Fig.2 Typical Decay Heat Curve Used in PWR FLECHT Test

Table 1 Summary of Run Conditions and Run Results

NO.	RUN NO.	BUNDLE SIZE	SYSTEM PRESSURE	PEAK POWER	INLET VEL.	INLET SUBCOOL-ING	INITIAL CLAD TEMP.	QUENCH TIME	QUENCH TEMP.	QUENCH VEL.	SUBCOOLING AT QUENCH
			KG/CM^2	KW/M	CM/S	°C	°C	SEC.	°C	CM/S	°C
1	0105	7 7	3.95	4.1	15.2	76	427	75	387	1.66	40
2	0307	7 7	4.08	4.1	25.0	77	654	50	442	3.37	53
3	0408	7 7	4.15	4.1	25.4	78	985	51	425	3.37	54
4	0509	7 7	4.08	4.1	25.2	76	1103	64	425	3.37	53
5	0610	7 7	5.20	4.1	14.7	77	762	104	487	1.30	36
6	0711	7 7	1.05	4.1	15.0	76	871	104	500	1.31	43
7	0812	7 7	1.05	4.1	15.0	76	986	105	449	0.86	43
8	0913	7 7	1.05	4.1	25.0	76	871	61	541	1.93	53
9	1002	7 7	3.94	4.1	15.2	76	874	76	431	2.05	40
10	1116	7 7	5.13	4.1	15.2	79	877	75	462	2.38	43
11	1314	7 7	4.01	4.1	14.7	105	873	65	533	2.33	67
12	1417	7 7	6.33	4.1	14.7	83	877	73	439	2.05	46
13	1615	7 7	2.11	4.1	14.7	72	878	105	446	1.35	36
14	1720	7 7	4.29	4.1	15.0	14	881	165	423	1.08	0
15	2322	7 7	1.05	4.1	10.2	82	881	185	482	0.60	33
16	3440	10 10	3.87	4.1	15.0	73	651	65	416	1.78	33
17	3541	10 10	4.01	4.1	15.0	78	870	71	400	1.76	39
18	3642	10 10	4.01	4.1	15.0	78	985	87	429	1.41	40
19	3724	10 10	4.01	4.1	4.8	78	642	175	421	0.70	0
20	3823	10 10	4.01	4.1	4.8	12	649	233	415	0.57	0
21	3920	10 10	3.87	4.1	14.7	9	876	162	396	1.22	0
22	4027	10 10	4.01	2.3	4.8	78	867	130	378	1.20	18
23	4129	10 10	4.22	4.6	4.8	74	869	224	454	0.56	0
24	4225	10 10	4.15	4.1	4.8	77	869	192	426	0.65	0
25	4321	10 10	4.08	4.1	10.0	78	873	102	434	1.14	22

Summary of Run Conditions and Run Results (cont'd)

NO.	RUN NO.	BUNDLE SIZE	SYSTEM PRESSURE	PEAK POWER	INLET VEL.	INLET SUBCOOL-ING	INITIAL CLAD TEMP.	QUENCH TIME	QUENCH TEMP.	QUENCH VEL.	SUBCOOLING AT QUENCH
			KG/CM^2	KW/M	CM/S	°C	°C	SEC.	°C	CM/S	°C
26	4442	10 10	4.15	4.1	14.7	77	989	74	429	1.73	37
27	4526	10 10	4.01	2.3	15.0	77	876	54	454	2.82	54
28	4628	10 10	4.15	4.6	15.0	83	874	71	458	1.59	39
29	4718	10 10	3.87	4.1	15.0	48	877	103	401	1.13	11
30	5019	10 10	3.87	4.1	25.0	9	874	118	415	0.83	0
31	5123	10 10	3.87	4.1	4.8	13	875	246	432	0.53	0
32	5231	10 10	1.27	4.1	15.0	29	873	170	284	0.49	0
33	5332	10 10	1.97	4.1	15.0	48	873	96	392	0.99	9
34	5433	10 10	5.00	4.1	15.0	87	879	61	431	2.33	47
35	5534	10 10	5.91	4.1	15.0	90	879	54	468	2.33	49
36	5642	10 10	4.22	4.1	14.7	78	988	75	408	1.71	38

2. Investigation of the Effects of Parameters on Film Boiling Heat Transfer Coefficients in PWR FLECHT[1] Test

2.1 Film Boiling Heat Transfer Region

The typical histories of the surface temperatures and the calculated heat transfer coefficients selected from the PWR FLECHT test[1] are illustrated in Figs. 3 and 4. The point Q where the surface temperature begins to fall steeply near to the saturation temperature is called as a quench point and the maximum temperature point P as a turnaround point in Fig. 3. With regard to quenches, their times and temperatures of 36 runs at the midplane of rods are listed in Table 1. From the quench times and the quench temperatures listed in Table 1, it is concluded that,

1°) Quench temperature is in general higher than 300°C (which is about equal to the Leidenfrost temperature). Soon after quench, the rod surface temperature becomes about saturation temperature of coolant as seen in Fig. 3. Then, the rod surface can not be wet with water stably and continuously before the occurrence of quench and on the other hand, the surface can be wet after quench.

2°) Quench occurs delaying from the time when the water level arrives the midplane of the rods, where the thermocouples are equipped for measurements.

3°) Judging from the facts described in 1°) and 2°), there exists the liquid in the vicinity of the heater rod surface above the quench point but the liquid does not touch the rod surface.

4°) Then, the quench point where the surface temperature falls steeply can be approximately considered as the start of the film boiling heat transfer region and whence on the rod surface above the quench, there exists the film boiling heat transfer region with some length.

5°) With regard to this film boiling, the flow model shown in Fig.5 is introduced as a conceptional diagram of flow.

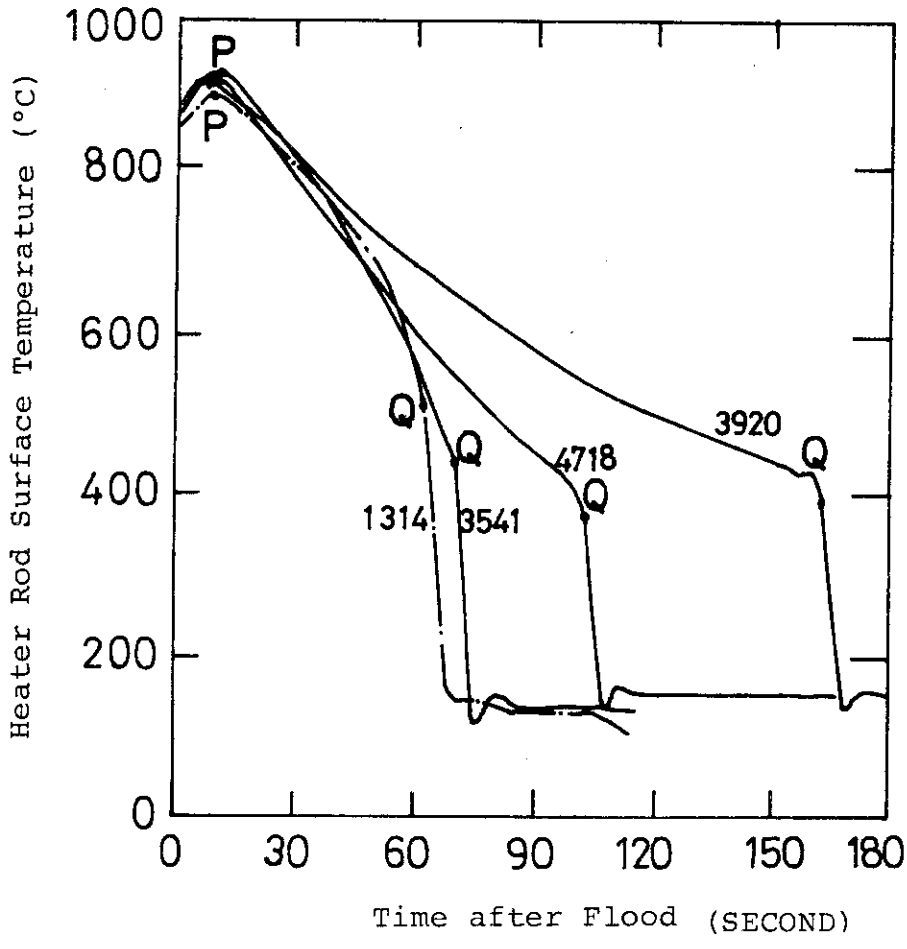

Fig.3 Typical Histories of the Surface Temperatures in PWR FLECHT Test

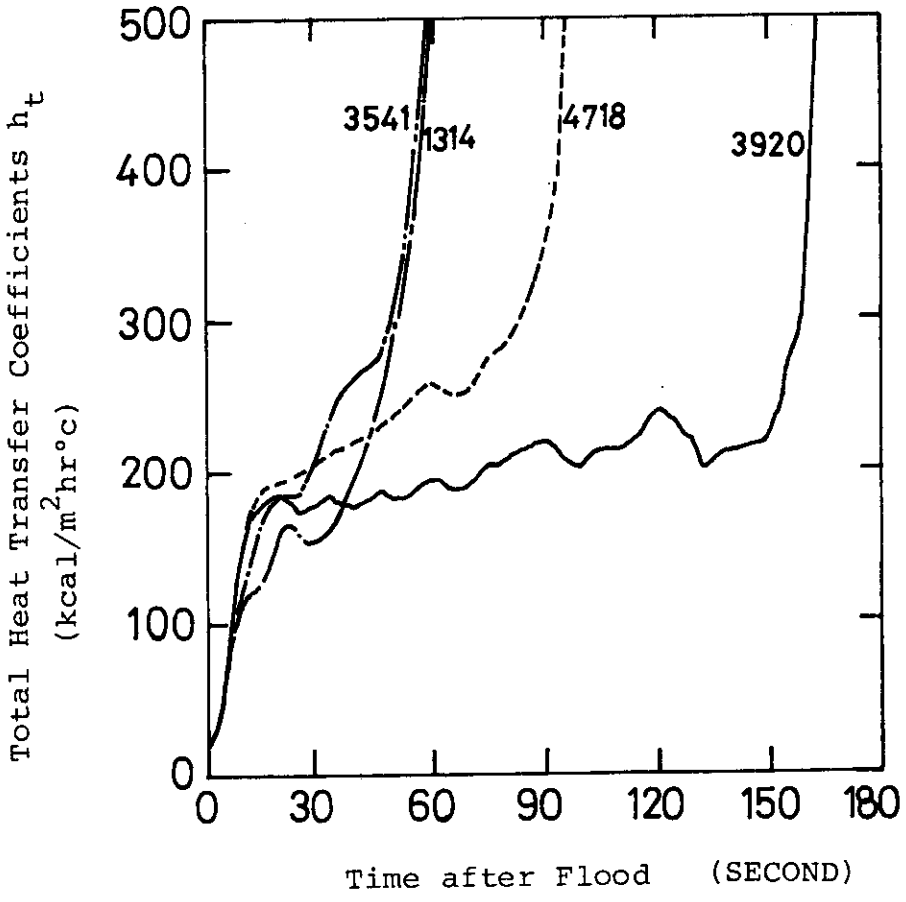

Fig.4 Typical Histories of the Total Heat Transfer Coefficients h_t in PWR FLECHT Test

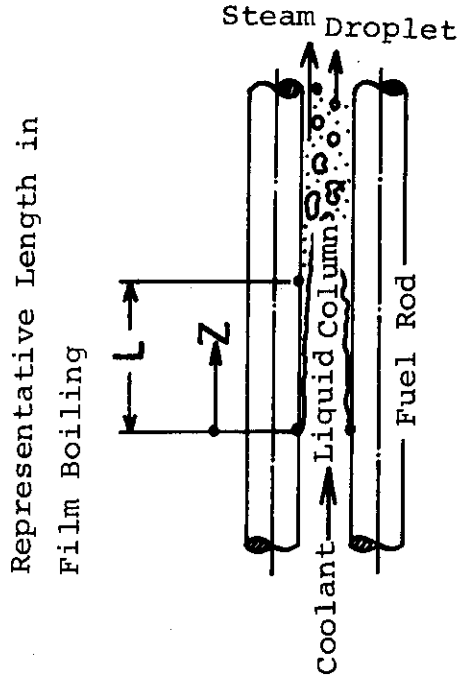

Fig.5 Flow Model as A Conceptional Diagram of Flow for Film Boiling Heat Transfer Region

2.2 Representative Length L with Film Boiling

Then, here the representative length L with film boiling is introduced. In Fig. 5, the length from the quench point Q to the point M where the thermocouple is equipped, can be considered as the representative length L. In this analysis, the point M corresponds to the midplane of the rod.

As the quench times t_{qu}, t_{qM}, t_{qB} at the elevation 8', 6', 4' from the lower end of the rod are known in PWR FLECHT test[1], the quench

velocity U_q at the midplane can be calculated as follows.

$$U_q \quad \{(\ell_u-\ell_M)/(t_{qu}-t_{qM}) + (\ell_M-\ell_B)/(t_{qM}-t_{qB})\{/2 \qquad (1)$$

where ℓ_u = 8', ℓ_M = 6' (midplane), ℓ_B= 4'. Quench velocities at each run are summarized in Table 1. Then, the length L can be approximately obtained as follows with U_q and the time t before quench occurs at the point M.

$$L = t \cdot U_q \qquad (2)$$

By adopting this representative length L, the heat transfer coefficients can be evaluated and the effects of various parameters on the heat transfer coefficients can be investigated even with the different conditions of parameters such as inlet subcooling, injected velocity and initial clad temperature.

2.3 Effects of the Inlet Subcooling, Injected Velocity, Initial Clad Temperature and System Pressure

The total heat transfer coefficients h_t shown in Fig. 4 are given as the sum of the convective term h_c and the radiative term h_r. The term h_r is dependent on the emissivity ε, rod surface temperature T_w and the saturation temperature T_s of water and is evaluated as

$$h_r = \varepsilon\sigma\{(\frac{T_w}{100})^4 - (\frac{T_s}{100})^4\}/(T_w - T_s) \qquad (3)$$

where σ is the Stefan-Boltzmann constant.

As the term h_r can be evaluated with $\varepsilon \simeq 1$ with considerably good accuracy, we will focus to the convective term h_c only. In the Figs. 6 ∿ 8, the heat transfer coefficients h_c at the midplane of the rods are illustrated with regard to the length L from the quench point to the midplane. In these figures, except for only one parameter the other run conditions are the same in order to investigate the effects of that parameter on the film boiling heat transfer coefficients. These data are calculated from the histories of the rod surface temperature T_w, the total heat transfer coefficients h_t at the midplane (6' elevation), quench velocity and system pressure using eqns. (1), (2) and (3).

(A) Effect of the Inlet Subcooling: The effect of the inlet subcooling are illustrated in Fig. 6. The conditions of the other parameters

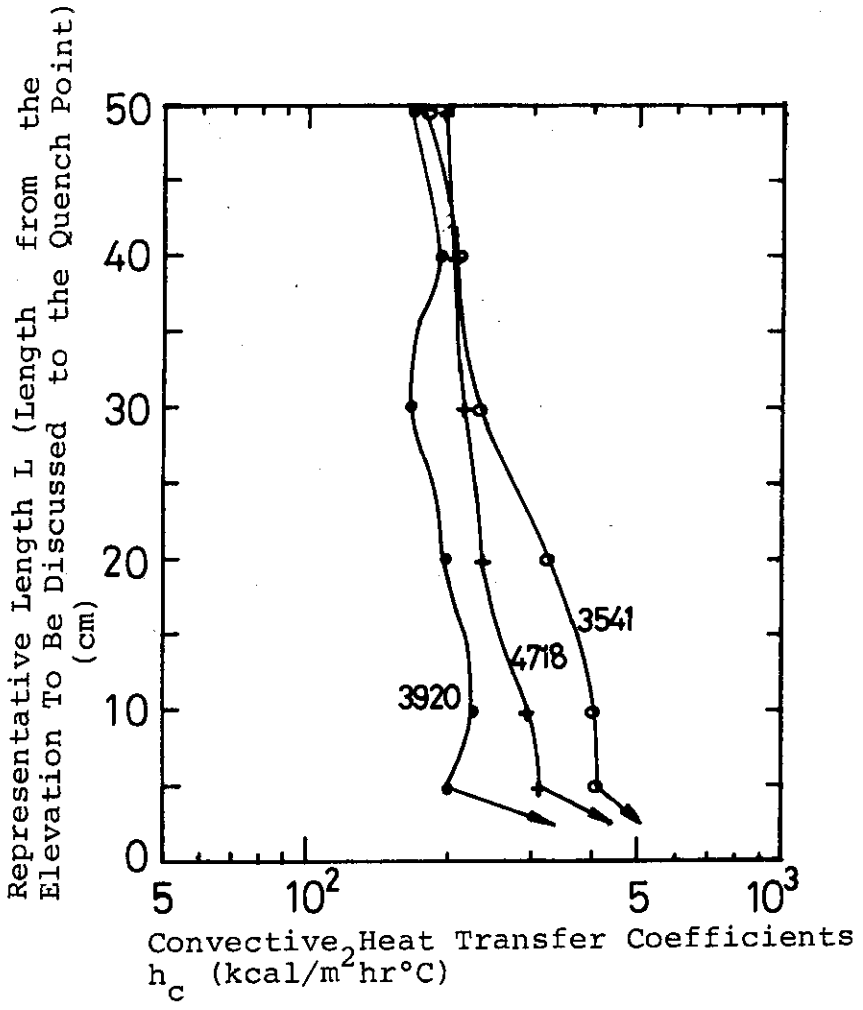

P=3.87-4.01 kg/cm² ab. U_{in}=14.7-15.0 cm/sec. $T_{w,int}$=870-877 °C.

Run No.	Inlet Subcooling (°C)
3920	9
4718	48
3541	78

Fig.6 (A) Effects of the Inlet Subcooling on Convective Heat Transfer Coefficients h_c in PWR FLECHT Test

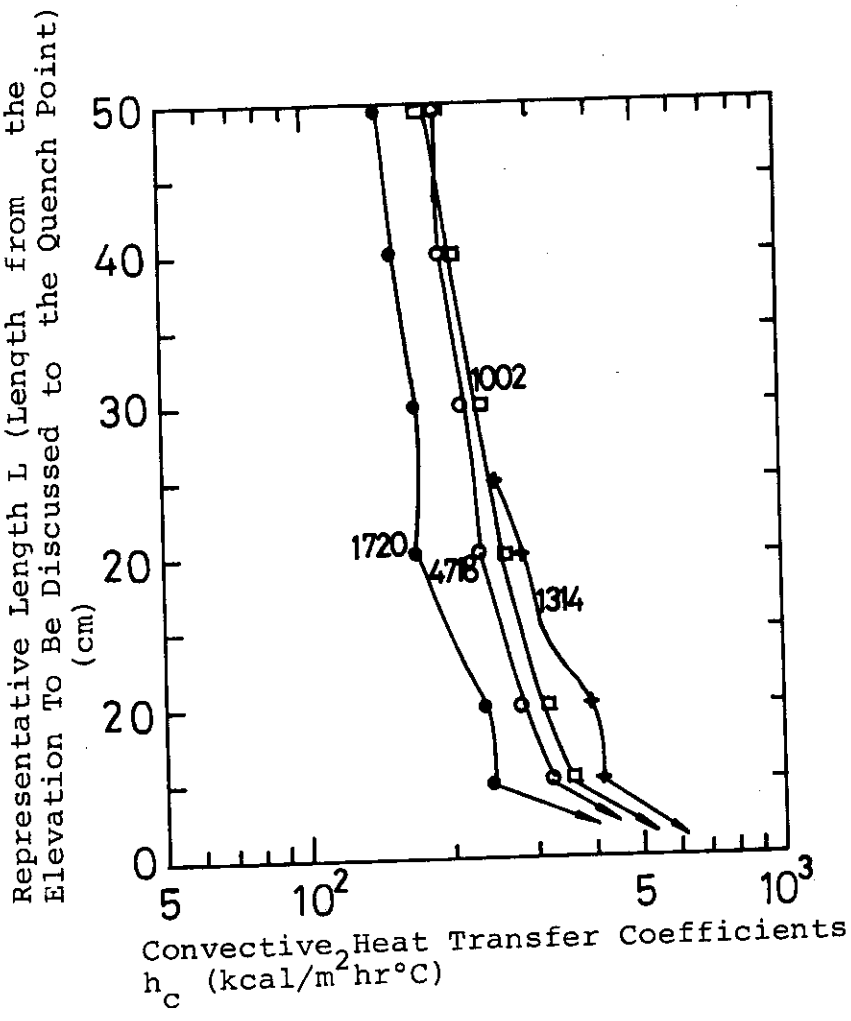

P=3.87-4.29 kg/cm^2 ab.
U_{in}=14.7-15.2 cm/sec.
$T_{w,int}$=873-881 °C.

Run No.	Inlet Subcooling (°C)
1720	14
4718	48
1002	76
1314	105

Fig.6 (B) Effects of the Inlet Subcooling on Convective Heat Transfer Coefficients h_c in PWR FLECHT Test

are the same and are shown in the title of the figure.

(1°) This figure indicates that the greater inlet subcooling gives the higher heat transfer coefficients h_c for the same length in the range from 0 cm to 40 cm long. As for the reason of this tendency, it can be considered that the local subcooling at the midplane would become large with increase of the inlet subcooling. Under the same conditions of the other parameters, the heat transfer from the vapour film into the liquid becomes greater in proportion to increase of the local subcooling ΔT_{sub}; ΔT_{sub} is defined as the difference of the saturation temperature T_s and the local liquid bulk temperature T_L. As the result, the vapour generation becomes smaller and then, the vapour film thickness δ_v becomes smaller. The heat transfer coefficients are expressed with the thermal conductivity k_v as $h_c = k_v/\delta_v$.

It follows that h_c becomes large with the small δ_v.

(2°) As the common tendency in each run, this figure also indicates that the larger length L gives the smaller magnitude of the heat transfer coefficients h_c.

(3°) The magnitude of the effect of the inlet subcooling on h_c becomes large when the length L is small (especially near the quench point). It could be said that the effects of the local subcooling are stronger with the shorter length L if the explanation described above in (2°) is reasonable.

(4°) On the other hand when the length L becomes larger than about 40 cm, h_c is almost the same within the error of experiment with whatever magnitude of inlet subcooling. As the reason for this, the following two are considered. (a) In the case that the length L is larger than 40 cm, the top of the liquid column shown in Fig. 5 may be below the midplane of the rod and whence in the vicinity of the midplane there does not exist the film boiling heat transfer region. There may exist the two phase flow cooling of steam and liquid droplets. That is, the length L = 40 cm means the maximum length of the film boiling region in this case. (b) When the length L becomes larger than 40 cm, the local subcooling at the midplane may be kept constant, in other words, the local bulk liquid temperature T_L becomes the saturation temperature T_s ($\Delta T_{sub} = 0$).

(B) Effect of the injected water velocity; In Figs. 7(A) and (B), the effect of the injected water velocity is illustrated. The other run conditions are shown in the title of the figures. These figures indicate

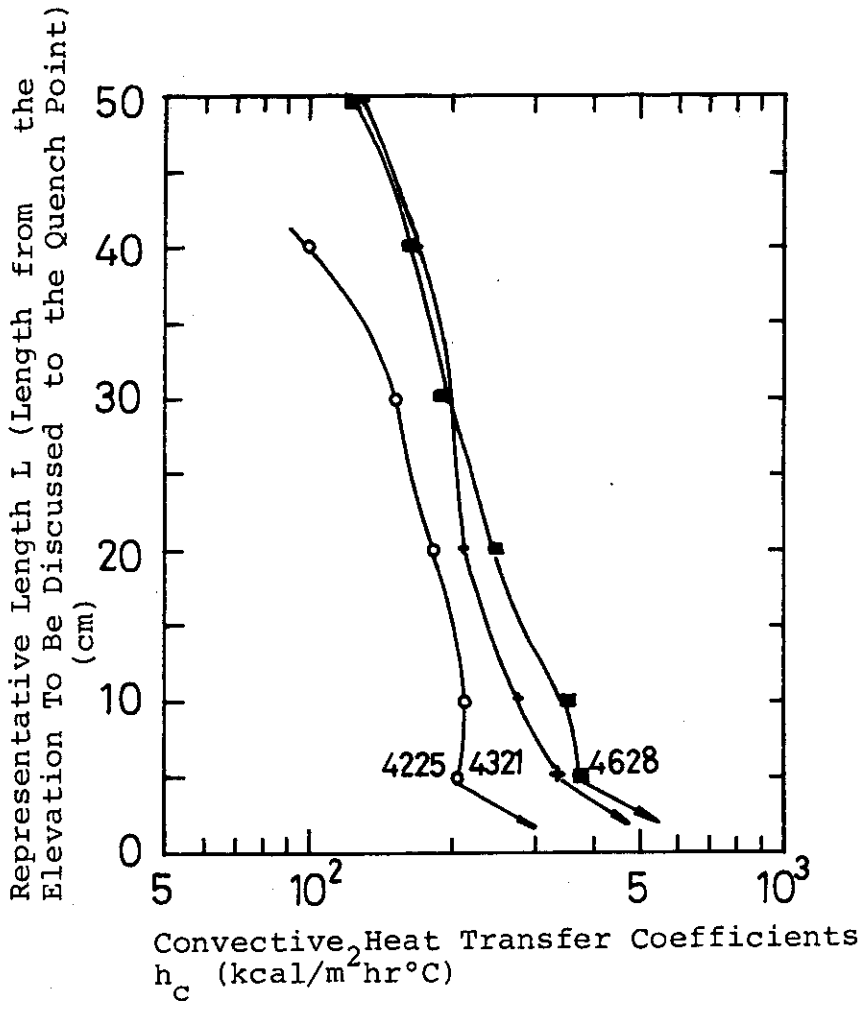

P=4.08-4.15 kg/cm^2 ab. $T_{sub,in}$=77-83 °C. $T_{w,int}$=873-869 °C.

Run No.	Inlet Velocity (cm/sec)
4225	4.8
4321	10.0
4628	15.0

Fig.7 (A) Effects of the Water Velocity U_{in} on Convective Heat Transfer Coefficients h_c in PWR FLECHT Test (P=4 ata)

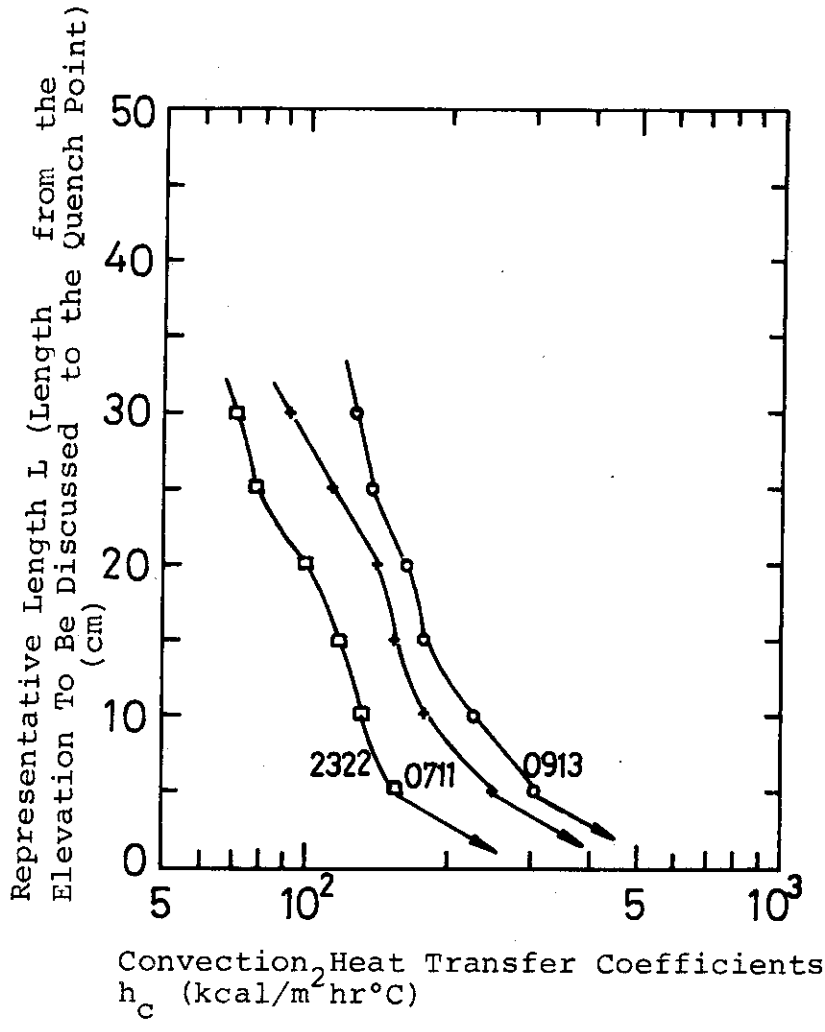

P=1.05 kg/cm^2 ab.
$T_{sub,in}$=76-82 °C.
$T_{w,int}$=871-881 °C.

Run No.	Inlet Velocity (cm/sec)
2322	10.2
0711	15.0
0913	25.0

Fig.7 (B) Effects of the Water Velocity U_{in} on Convective Heat Transfer Coefficients h_c in PWR FLECHT Test (P=] ata)

that the higher injected water velocity gives the larger heat transfer coefficients h_c with the same length L. Fig. 7(A) shows the case that the system pressure P is equal to 4 kg/cm^{2}ab and Fig. 7(B) the case that P is equal to 1 kg/cm^{2}ab. As the inlet subcooling and the power are almost the same with each run in Figs. 7(A) and 7(B), the local subcooling at the midplane is directly due to the magnitude of the injected water velocity, that is, the higher injected water velocity gives the larger local subcooling. Then, the effect of the injected water velocity does in this way cause the difference of the local subcooling of water at the midplane.

(C) Effect of the initial clad temperature $T_{w,int}$; The effect of the initial clad temperature $T_{w,int}$ is shown in Figs. 8(A) and 8(B). The initial clad temperature $T_{w,int}$ is the one at the midplane at the time when the water starts to be injected into the test section. From the figure, a very interesting and important fact can be pointed out that the heat transfer coefficients h_c are almost the same within the error of experiments with the same length L under whatever conditions of $T_{w,int}$. The effect of T_w itself is diminishing tactfully because the heat transfer coefficients h_c are obtained by substracting the radiative term h_r from the total heat transfer coefficients h_t, where h_r is directly dependent on the rod surface temperature $T_{w(t)}$. It is made clear from this presentation of heat transfer coefficients that the initial clad temperature $T_{w,int}$ are not necessary to be paid attention to on purpose to evaluate the coefficients h_c. In addition, it can be guessed that the local water subcooling is not affected significantly at the midplane with the differences of $T_{w,int}$ because the much time elapses before the film boiling region appears in the vicinity of the midplane and because the effects of the initial clad temperature $T_{w,int}$ has diminished already.

(D) Effect of the system pressure P; In the Figs. 7(A) and 7(B), the effect of the system pressures p 4 ata and p 1 ata can be compared with regard to the parameter of the injected water velocity. Although the test runs are done in small numbers, the effect of the system pressure P appears on the heat transfer coefficients h_c, that is, the higher system pressure gives the larger heat transfer coefficients h_c with the same length L under the same injected water velocity condition. This tendency would be reasonably understood from the relation of $h_c = k_v/\delta_v$. For, the specific weight γ_v of steam becomes larger and then the vapour film thickness δ_v becomes smaller when the system pressure p becomes larger, on the other

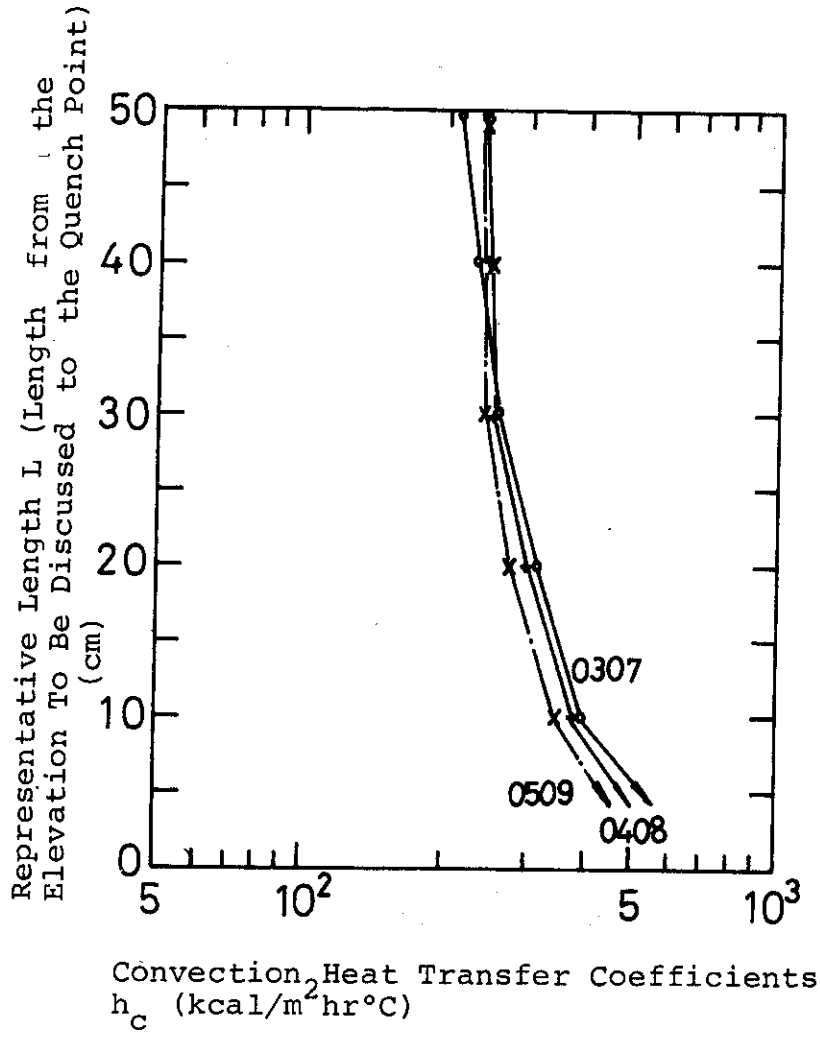

P=4.08-4.15 kg/cm² ab. U_{in}=25.0-25.4 cm/sec. $T_{sub,in}$=76-78 °C.

Run No.	$T_{w,int}$ (°C)
0509	1103
0408	985
0307	654

Fig.8 (A) Effects of the Initial Clad Temperatures $T_{w,int}$ on Convective Heat Transfer Coefficients h_c in PWR

(U_{in}=25 cm/sec)

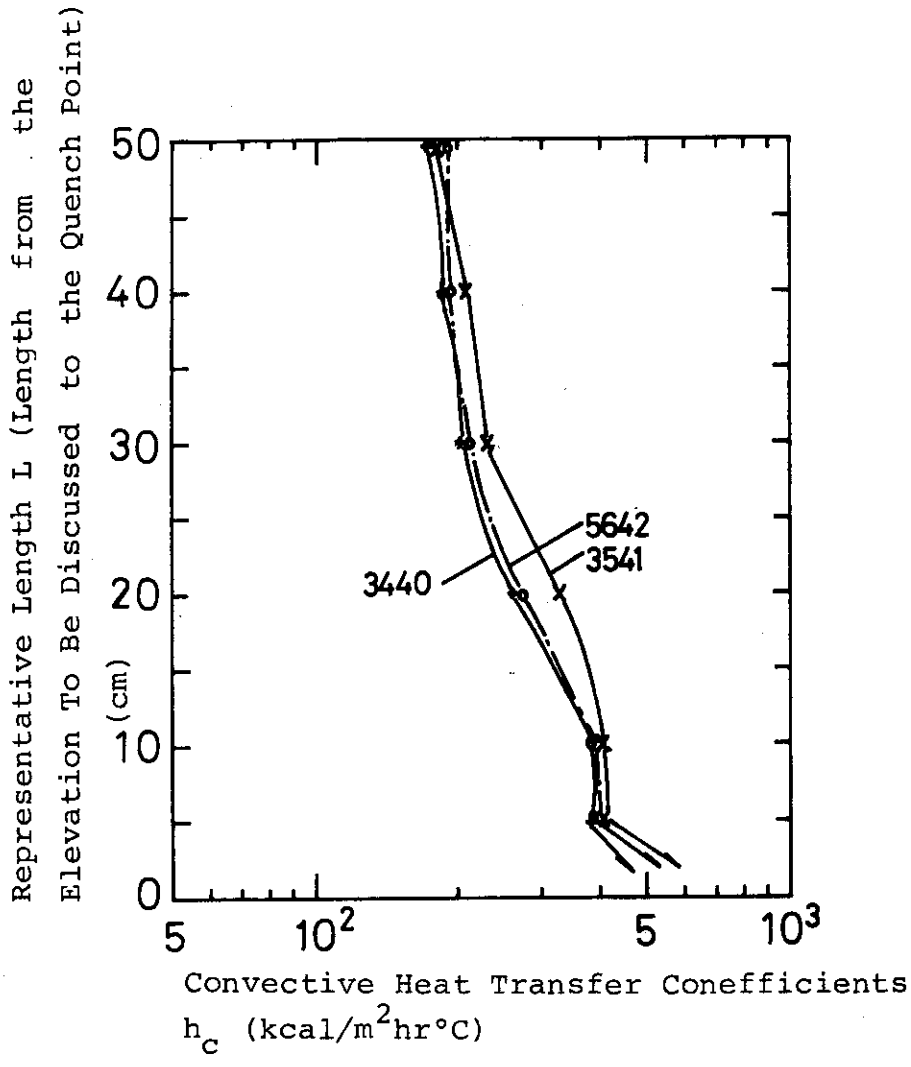

P=3.87-4.22 kg/cm^2 ab.
U_{in}=14.7-15.0 cm/sec
$T_{sub,in}$=73-78°C

Run No.	$T_{w,int}$(°C)
5642	988
3541	870
3440	651

Fig.8 (B) Effects of the Initial Clad Temperatures $T_{w,int}$ on Convective Heat Transfer Coefficients h_c in PWR FLECHT Test (U_{in}=15 cm/sec)

hand, the thermal conductivity k_V is almost the same. In this way, with regard to the other parameters, the same tendency on the effect of the system pressure is to be observed from the same reason.

2.4 Summary of the Effects of Inlet Subcooling, Injected Water Velocity, Initial Clad Temperature and System Pressure

The data presentation that the heat transfer coefficients h_c are related with the film boiling length L from the quench point to the midplane, can make clear the effects of the main parameters which would not be understood from the data presentation that the total heat transfer coefficients h_t are related with time after flooding. That is, with the same condition of the other parameters,

(1°) The larger inlet subcooling gives the larger heat transfer coefficients h_c for the same length L of film boiling.

(2°) When the injected water velocity is larger, h_c becomes larger with the same length L.

(3°) When the initial clad temperature is higher, h_c is almost the same within the error of experiments with the same length L.

(4°) It is pointed out that the higher system pressure gives the higher heat transfer coefficients h_c with the same length L although the test runs are in small numbers.

(5°) In each run, h_c becomes smaller as the length L becomes larger.

By the way, as regards the inlet subcooling the liquid bulk temperature T_L at the midplane may reach the saturation temperature T_s by receiving the heat from the rod surface until the water reaches the midplane of the rod in case of low injected water velocity even if the inlet subcooling is large. On the contrary, even if the inlet subcooling is rather low, T_L at the midplane can be fully below the saturation temperature T_s in case of high injected water velocity. Accordingly, only when the other parameters are the same the effect of one parameter, for example the inlet subcooling or the injected water velocity can be independently discussed, but when another parameter, for example, the injected water velocity is different the local subcooling at the midplane can not be decided in proportion to the inlet subcooling. For, the local subcooling is decided at the same time from the inlet subcooling, injected water velocity and heat output from the rod surface. As has been investigated in section 2.3, the effects of both

the inlet subcooling and the injected water velocity should be evaluated at the same time and systematically by introducing the local subcooling at the midplane. Then, in order to evaluate the effect of the local subcooling on h_c precisely the local subcooling is first to be evaluated at the midplane. In other words, when the conditions are quite different, h_c can not be soon evaluated even if only the effect of the inlet subcooling on h_c has been estimated from the test runs with the same conditions of the other parameters and that, it follows that the effects of the local subcooling can not be also evaluated so far as the local subcooling has not been decided at the midplane.

3. Estimation of the Local Subcooling at the Midplane and It's Effect on h_c

3.1 Estimation of the Local Subcooling at the Midplane

In this section the local subcooling at the midplane is estimated. When water rises along the vertical heater rods, the quench points move upwards on the rod surfaces behind time with the velocity smaller than the inlet water velocity U_{in}. As seen in Fig. 3, the rod surface temperature is at most the saturation temperature T_s below the quench point. Then, it could be said that the heat output from the rod surface is consumed to rise the water temperature T_L along the rod below the quench point. The local subcooling of water at the midplane at the time when the midplane quenches, is decided from calculating the temperature rise ΔT_L between the lower end of the heater rod and the midplane. The heater rod has the power distribution η_n along its increment length ℓ_n as shown in Fig. 1 and power change $\xi(t)$ with time after flooding is also shown in Fig. 2. The power change $\xi(t)$ simulates the decay heat curve. The initial heat flux Q_{no} in each increment ℓn is shown as $\eta_n \cdot Q_o$ with the initial heat flux Q_o at the midplane. The heat flux $Q_{n,t}$ at the time t in each increment is shown as

$$\xi(t)Q_{no} = \xi(t)\cdot\eta_n\cdot Q_o \quad .$$

It is assumed here that all of the heat generation in the increment is consumed to rise the temperature of water while the water passes through the increments. Then, the temperature rise ΔT_{Ln} of water in the increment ℓn is expressed as follows with the time t_n, where t_n is the time that after flood the water reaches the midplane of the increment ℓ_n.

$$(D^2 - \frac{\pi}{4} d^2)\gamma_L C_p \Delta T_{Ln} = \frac{1}{3600} \pi d \xi(t_n) \eta_n Q_o \frac{\ell n}{U_{in}} \qquad (4)$$

where D is the heater rod pitch (m), d the diameter of rod (m), γ_L the water density (kg/m^3), ℓ_n the increment length (m), C_p specific heat of water (kcal/kg°C), Q_o the initial power at the midplane ($kcal/m^2hr$) and U_{in} the injected water velocity (m/sec).

When the water passes from the 1st increment to the Nth increment, the sum ΔT_Σ of the temperature rises ΔT_{Ln} during each increment is expressed as below.

$$\Delta T_\Sigma = \sum_{n=1}^{N} \Delta T_{Ln} = \frac{\pi d Q_o}{3600(D^2 - \frac{\pi}{4} d^2)\gamma_L C_p U_{in}} \sum_{n=1}^{N} \xi(t_n)\eta_n \ell_n \qquad (5)$$

To evaluate the right-hand side of Eqn. (5), the time t_n in Eqn. (5) is necessary to be decided. The time ℓ_M/U_{in} elapses for the water to reach the midplane from the lower end of the heater rod, where ℓ_M is the length between the two and U_{in} the water velocity. The water existing in the vicinity of the midplane at the time t_Q when the midplane quenches, has been injected at the time $(t_Q - \ell_M/U_{in})$ after flood. Then, t_n which is the time after flood when this water reaches the midplane of the increment ℓ_n is expressed as follows.

$$t_n = t_Q - \frac{\ell_c}{u_o} + (\frac{n}{2} + \sum_{i=1}^{n-1} \ell_i)/u_o \qquad (6)$$

The value of $\xi(t_n)$ corresponding to the time t_n is evaluated from Fig. 2. Then, the right-hand side of Eqn. (5) is evaluated from Table 1, Figs. 1 and 2, rod configuration and the physical properties of water. The local subcooling ΔT_{sub} of water in the vicinity of the midplane at the quench time t_Q are approximately shown as

$$\Delta T_{sub} = \Delta T_{sub,in} - \Delta T_{\Sigma} \quad . \qquad (7)$$

Although the local subcooling at the midplane corresponding to the value of L can not be, of course, expressed with Eqn. (7) precicely, the local subcooling in the vicinity of the midplane can be evaluated with considerably good accuracy so far as the values of L and L/U_{in} are not too large. The local subcooling at the midplane at the time t_Q in each run is shown in Table 1. When the subcooling is zero, the film boiling is the saturated one. When it is not zero, that is the subcooled one.

3.2 Saturated Film Boiling Heat Transfer

In Fig. 9, the heat transfer coefficients h_c in all cases of the test runs of saturated film boiling are shown with regard to the length L. Except for two runs 3823 and 5123, the heat transfer coefficients h_c are scattering in a certain band with the same length L and the tendencies of h_c with the length L are similar to each other runs. With respect to the runs 3823 and 5123, the water temperature T_L becomes the saturated one T_s soon after flood, that is, at the elevation much lower than the midplane of rod. Then, the fluid at the midplane at the time t_Q must be the two-phase flow certainly. Then, its heat transfer characteristics are considered to be different from the saturated film boiling. Also with respect to the other

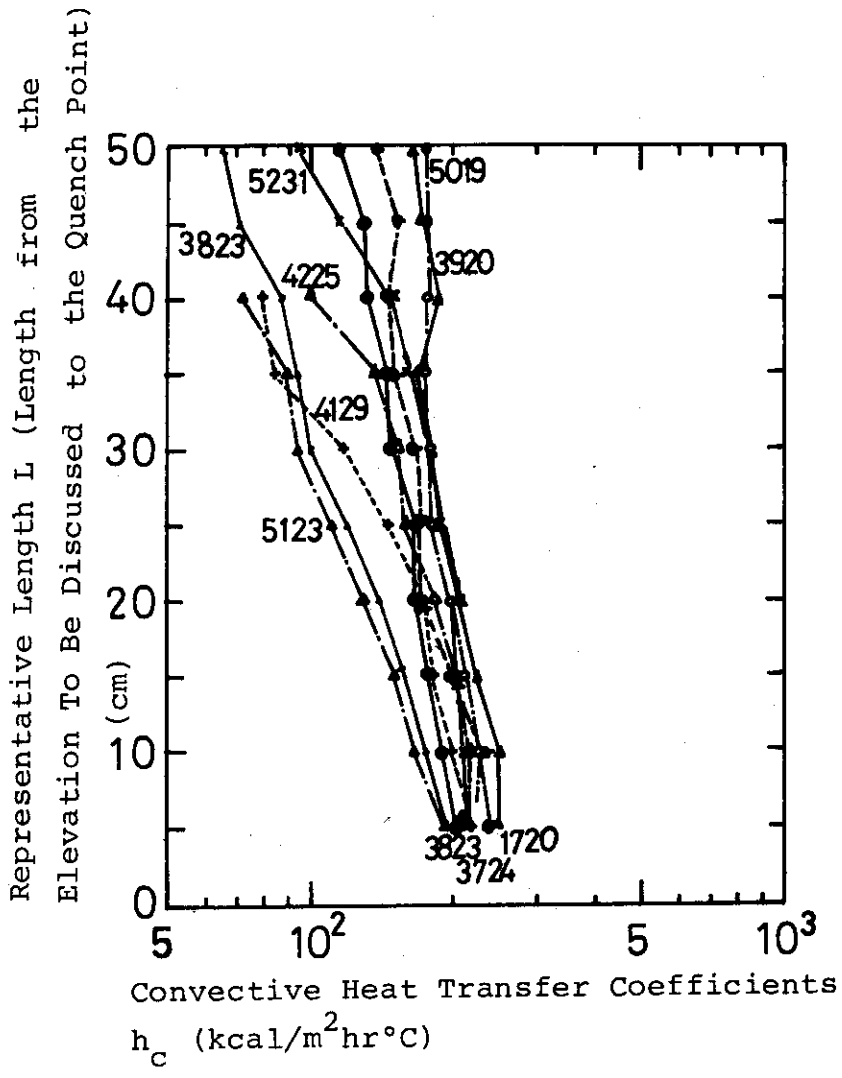

Fig.9 Saturated Film Boiling Heat Transfer Coefficients $h_{c,sat}$ inPWR FLECHT Test

seven runs, the band in which the data are scattering becomes much wider with the length L larger than 35 ∿ 40 cm. This reason is due to the same one described above, that is, when the length L becomes larger than 35 ∿ 40 cm, the film boiling region ends and two phase flow consisted of steam and water droplets occurs. When this two phase flow exists, the heat transfer characteristics are dependent on another new parameter, quality or void fraction. If the length L is restricted less than 35 ∿ 40 cm, the saturated film boiling heat transfer coefficients $h_{c,sat}$ are very well understood with the length L.

3.3 Subcooled Film Boiling Heat Transfer

The heat transfer coefficients h_c in all the other cases of the runs where the local subcooling T_{sub} is not zero are shown in Figs. 10(A) and 10(B) by taking ΔT_{sub} and pressure P as the parameters with regard to the film boiling length L. Fig. 10(A) shows the case of constant pressure P 4 ck/cm^{2}ab with various local subcoolings and Fig. 10(B) the case of constant local subcooling ΔT_{sub} 35°C with various pressures. In Figs. 10(A) and 10(B), it can be soon understood that the relation between h_c and L has the systematic tendency with regard to L and to ΔT_{sub} in all seven test runs although the run conditions are much different to each other. h_c becomes larger as the local subcooling ΔT_{sub} becomes larger with the same length L and so does it with the larger pressure under the same local subcooling.

3.4 Summary of Characteristics of Film Boiling during REflood

(1°) The film boiling during reflood is characterized by the process in which the coolant is supplied upwards along the high temperature vertical full rods and by the phenomena that this region moves upwards later than the water rises upwards along the rods.

(2°) As the representative length of the film boiling during reflood, can be selected the length L in the film boiling region from the quench point to the elevation to be discussed.

(3°) Especially as the characteristics of the film boiling heat transfer coefficients h_c, it can be pointed out that the inlet subcooling and the injected water velocity have a great influence on h_c as the effect of the local subcooling in the film boiling region.

Then, the following two steps are to be taken; h_c is to be evaluated first of the saturated film boiling (i.e. $\Delta T_{sub} = 0$) and second, h_c of the subcooled film boiling with the local subcooling ($\Delta T_{sub} > 0$).

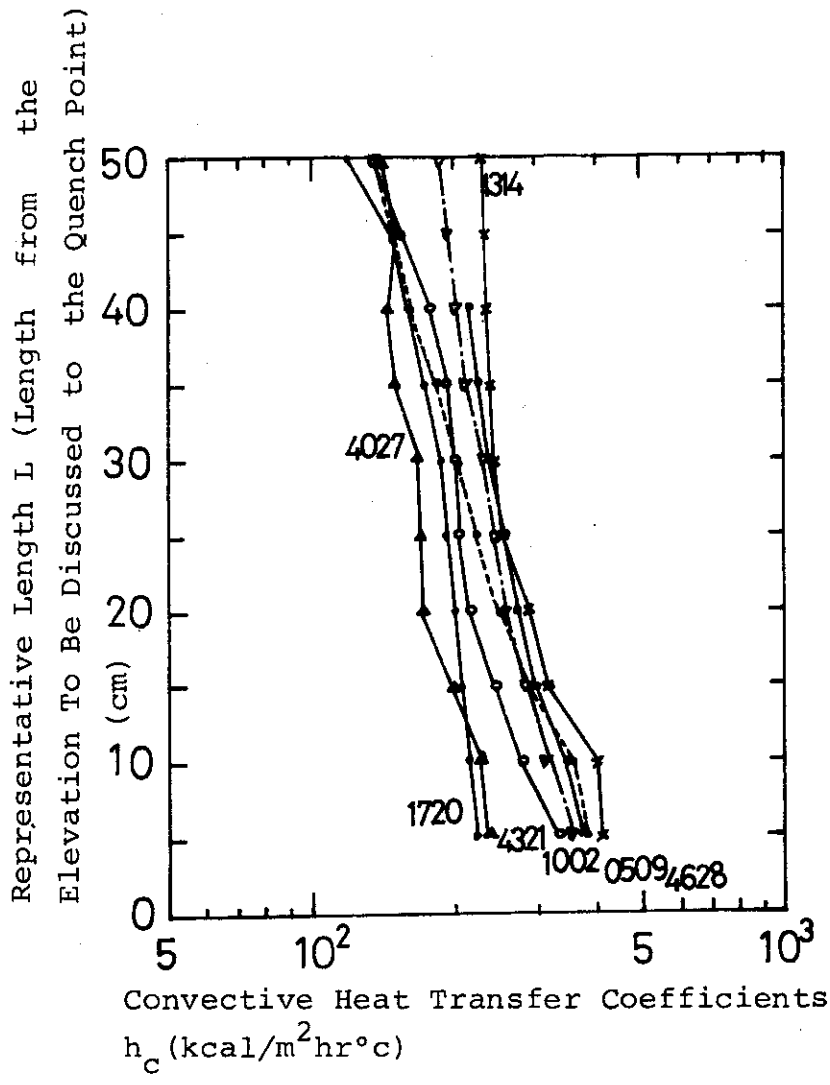

Run No.	ΔT_{sub} (°C)	Pressure (kg/cm^2)
1720	0	4.29
4027	18	4.01
4321	22	4.08
1002	40	3.94
4628	39	4.15
0509	53	4.08
1314	67	4.01

Fig.10 (A) Subcooled Film Boiling Heat Transfer Coefficients $h_{c,sub}$ in PWR FLECHT Test (P=4 ata)

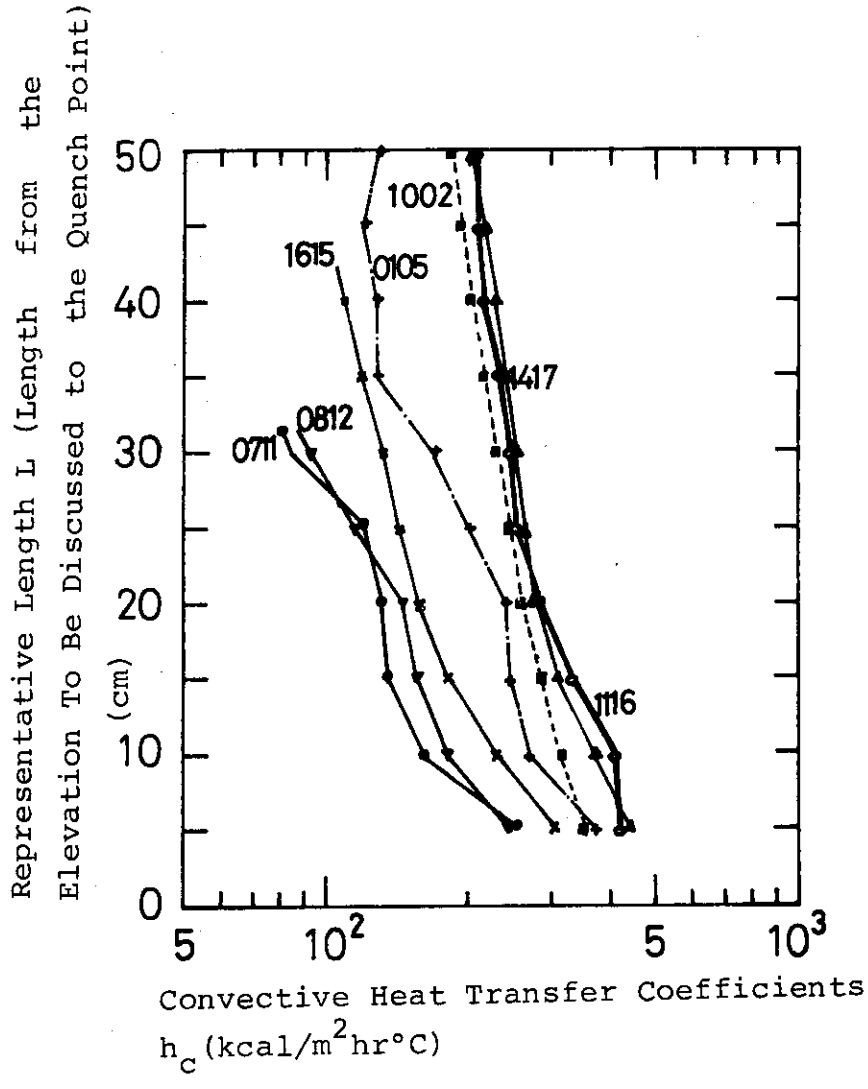

Run No.	T_{sub}(°C)	Pressure(kg/cm^2)
0812	43	1.05
0711	43	1.05
1615	36	2.11
0105	40	3.95
1002	40	3.94
1116	43	5.13
1417	46	6.33

Fig.10 (B) Subcooled Film Boiling Heat Transfer Coefficients $h_{c,sub}$ in PWR FLECHT Test; Effects of the System Pressure

4. Relation of the Film Boiling during Reflood with Previous Studies on Film Boiling

4.1 Previous Studies on Film Boiling

The studies on film boiling carried out previously are summarized as follows.

(I) Steady-state film boiling;

forced convection	vertical heater rod Ellion[2], Bromley[3],
	horizontal heater rod Chang[2], Berenson[5], Zuber[6], Sparrow & Cess[7],
natural convection	vertical heater rod Bromley[8], Hsu & Westwater[9]
	horizontal heater rod Tachibana[10], Bromley[11]

(II) Transient film boiling;
Tachibana et al.[12], Ishigai et al.[13]

As one of the previous film boiling studies which are intimately related to the film boiling during reflood, the one by Ishigai et al.[13] may be pointed out. In that, the flow observation and the temperature histories were investigated on the high temperature rod (10 cm long and 10 mm in diameter) thrown in the water pool. But even this case can't be directly applied to the film boiling during reflood because the test piece was too small and did not have the heat generation in itself.

Although the steady state film boiling studies can not be directly applied to, the film boiling during reflood has the possibility that it can be treated at least under quasi-steady state because the injected water velocity is at most about 25 cm/sec in the core and that, because the film boiling region moves with the velocity much less than that. When the previous studies on steady state film boiling are investigated from these viewpoints, the important and interesting facts are revealed as follows with regard to the effects of the representative length L, rod surface temperature T_w, water subcooling ΔT_{sub} and velocity V.

(1°) Representative length L; Bromley[8] analyzed the saturated film boiling heat transfer coefficients h_c on the vertical rod surface and introduced the following relation.

$$h_c = C\left[\frac{k_v^3 \gamma_v (\gamma_L - \gamma_v)(H_v - H_L)}{L\mu_v (T_w - T_s)}\right]^{1/4} \tag{8}$$

Bromley argued that the value of c is between 0.667 and 0.943 theoretically. Later, Ellion[2] selected 0.714 as C from experiments. His experiments were carried out under the condition; v = 1.1 ∿ 5 ft/sec, $\Delta T_{sub,in}$ = 50 ∿ 100 °F, P = 16 ∿ 60 psia.

These results imply that h_c becomes smaller as the length L becomes larger and that the effects of the water velocity V can be neglected in the velocity range described above.

(2°) Coolant velocity V; Bromley[3] estimated the effects of the coolant velocity V in the saturated steady-state film boiling on h_c from the investigation of the experiments in which water flows right to the horizontal heater rods of diameter D.

$$h_c = 0.62\left[\frac{k_v^3 \gamma_v \gamma_L (H_v - H_L)}{D\mu_v (T_w - T_s)}\right]^{1/4} \quad \text{when } V/\sqrt{gD} < 1.0 \tag{9}$$

$$h_c = 2.7\left[\frac{Vk_v \gamma_v (H_v - H_L)}{D(T_w - T_s)}\right]^{1/2} \quad \text{when } V/\sqrt{gD} > 2.0 \tag{10}$$

Although the case of the vertical heater rod is apparently different from the horizontal one in respect of the flow patterns, this experimental results are to be paid attention to because these imply at least the tendency of the effect of coolant velocity V on h_c.

(3°) Coolant subcooling; Rare are the studies which investigated the effects of the coolant subcooling ΔT_{sub} even in steady-state film boiling both experimentally and theoretically. With the subcooled water, the heat transfer will occur in the liquid phase and then, the heat transfer rate becomes larger compared with the case of saturated water.

Tachibana et al.[10] did the experiments with electrically heated nichrome wire of 0.5 mm and 0.8 mm in diameter set in water, alcohol and CCl_4 pools. The part of the results is illustrated in Fig. 11. They revealed that with the water subcooling of 45°C h_c becomes twice of the saturated film boiling heat transfer coefficients.

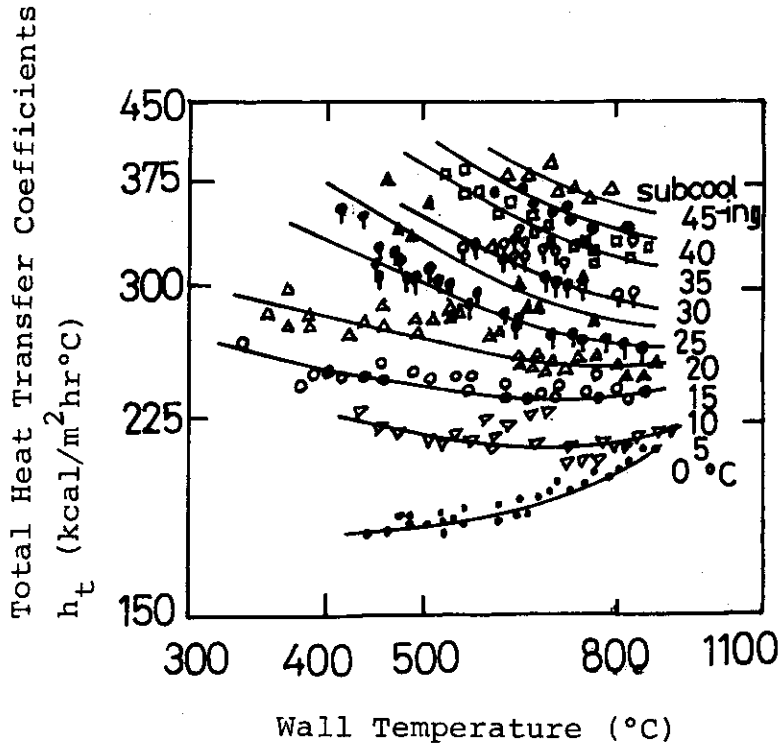

Fig.11 An Example of Effects of Water Subcooling on Heat Transfer Coefficients (after F.Tachibana et al)

4.2 Recent Studies on Film Boiling Heat Transfer during Reflood

(1) Uchida, Kaminaga et al.[16] carried out the fundamental experiment of reflood with the annular flow type test section which has the single heater rod in it and also studied the characteristics of the turnaround time, turnaround temperature, quench time and quench temperature as well as the observations of the flow. Kaminaga[17] presented the correlation of film boiling heat transfer coefficients,

$$h = c\left[\frac{k_v \gamma_v \gamma_L h'_{fg}}{L\mu_v (T_w - T_s)}\right]$$

$$c = 0.8 + 0.024 U_{in}^{1.6}$$

where U_{in} is the injected water velocity. The characteristics of his correlation is that the coefficient c is related only to the injected water velocity U_{in}. The principal aim of his analysis was to make clear the mechanism of the quench propagation and whence, the correlation of the film boiling heat transfer coefficients were used for this purpose. Then, this correlation is not always apply widely to the film boiling heat transfer during reflood and is rather to be used in the vicinity of the quench point. When this correlation is used in the developed film boiling region, the heat transfer coefficients are evaluated too high. As seen from the value c calculated as bellow, the coefficients h_c become twice or thrice too high when U_{in} is above 10 cm/sec.

U_{in} = 1 cm/sec, c = 0.823
U_{in} = 5 cm/sec, c = 1.102
U_{in} = 10 cm/sec, c = 1.716
U_{in} = 20 cm/sec, c = 3.576

Then, his correlation is to be restricted in any sense in order to be used as the film boiling heat transfer coefficients during reflood.

(2) Aoki et al.[18] also studied the film boiling heat transfer coefficients as well as the characteristics of the quench phenomena. They reported that the film boiling heat transfer coefficients lay in the band of 100 ∿ 200 kcal/m^{2}hr°C.

5. Film Boiling Heat Transfer Experiment

5.1 Experimental Apparatus

The schematic figure of the test rig is shown in Fig. 12.

The experimental apparatus is composed of the test section containing in it a vertical simulated heater rod and a recirculation water line through which water is supplied to the test section.

(1) Heater rod; The heater rod is made of the stainless steel tube - 6.2 mm I.D., 10 mm O.D. and 900 mm in effective heated length. On the surface of the rod five alumel-chromel thermocouples are furnished at the elevations 20, 40, 45, 50, 70 cm apart from the bottom of the effective heated section. The heater rod is directly heated by DC electric source. Both voltage and current are continuously recorded on the photographic paper at the same time with the heater rod temperature histories.

(2) Flow tube; Water is injected in the annular space between the flow tube and the heater rod at the bottom. The hydraulic diameter of the flow tube is rather equal to that of the fuel assembly of PWR. The broader flow tubes are used to compare the flow patterns and heat transfer characteristics.

(3) Thermal insulation tube; In the thermal insulation glass tube outside the flow tube, water is filled and it is held at the same temperature as the injected water's so as both to keep constant the wall temperature of the flow tube and to prevent the injected water from boiling on the flow tube wall.

5.2 Experimental Procedure

While the water is circulated through the recirculation line with pump, the temperature of the water in the reservior is regulated with the heater before the onset of an experiment. The water in the thermal insulation tube is also kept at the same temperature as the water in the reservoir with the heater in it. The electric power is supplied to the heater rod at the constant rate set beforehand. When the heater rod temperature reaches the value selected, the water is injected upwards the flow tube by actuating the valves and the run begins.

The injected water velocity U_{in} is calculated from the time that the level of the water rises up to the upper end of the unheated section of the

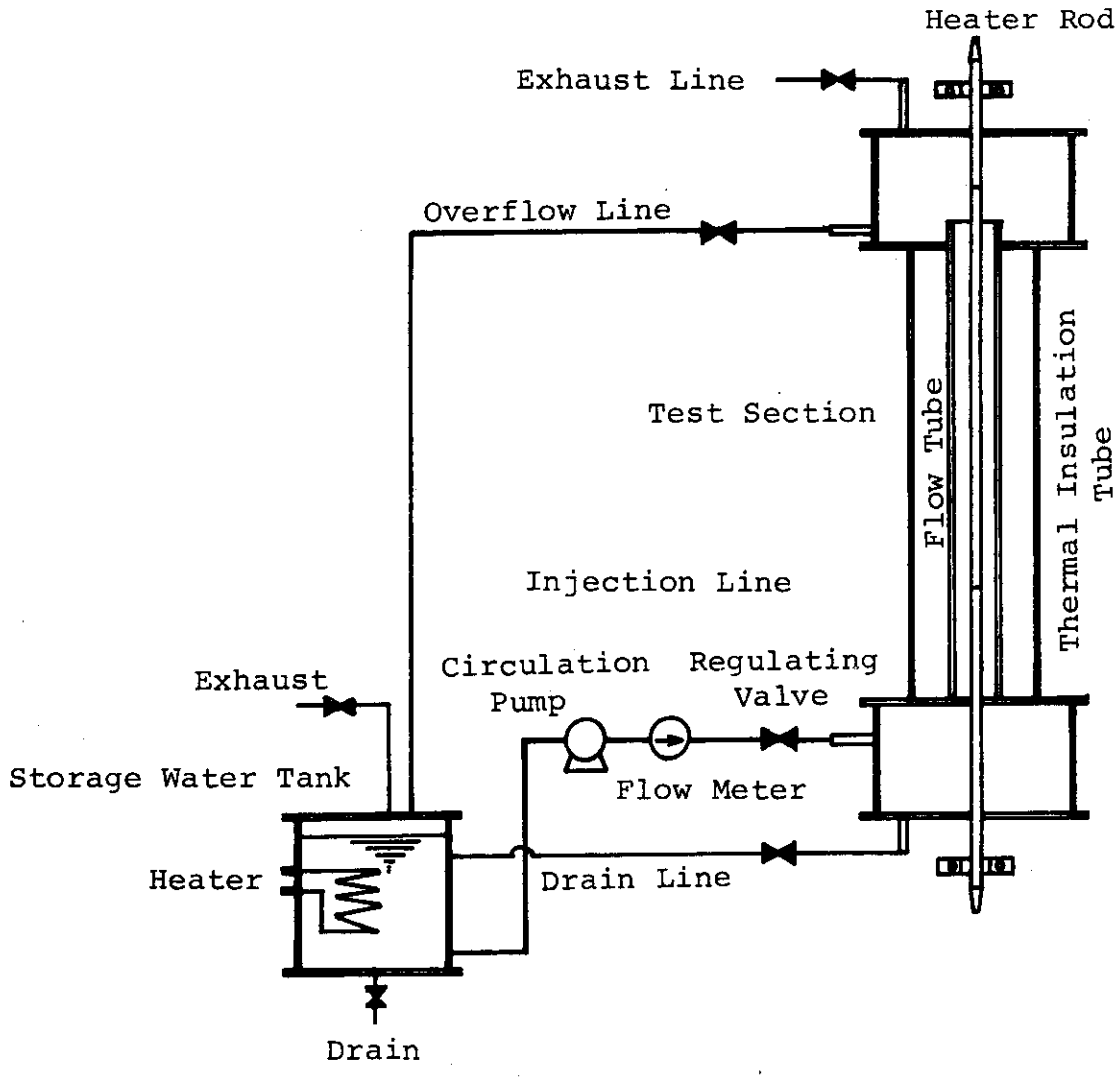

Fig.12 Schematic Figure of the Single Rod Experiment

heater rod, and water temperature T_{in} is measured at just before the inlet of the test section. In each run, temperature histories of the heater rod are continuously recorded as well as the voltage and current. The flow patterns are taken by photographs simultaneously.

5.3 Physical Parameters and Their Ranges

In the experiment, the main physical parameters and their ranges are as follows;

(1) injected water velocity U_{in}: 0.5 ∿ 30 cm/sec
(2) injected water temperature T_{in}: 20 ∿ 97 °C
(3) system pressure P : atmospheric pressure
(4) supplied electric power Q: up to 8 kw/m
(5) initial heater rod temperature $T_{w,int}$: 300 ∿ 950 °C

5.4 Validity and Advantage of Film Boiling Experiment by Annular Flow Type Test Section

In this experiment, the annular flow type test section is adopted to investigate the flow patterns and the heat transfer characteristics especially of the film boiling heat transfer region in the core of PWR. The configuration of the flow channels in the actual core is such as shown in Fig. 13(A) and there does not exist the outer wall of the annular flow type test section. As the means to simulate the flow channels shown in Fig. 13(A), such two types are considered as shown in Figs. 13(B) and (C), that is, single flow tube type and the annular flow tube type. The former simulates the unit of flow channels which is enclosed by four fuel rods and has the defect that the flow channel is all enclosed with the heated wall. Furthermore, it has the defect that the flow patterns can not be observed directly corresponding to the heat transfer characteristics. This study aims to evaluate the heat transfer coefficients in the film boiling heat transfer.

In this sense, it is necessary to observe the flow patterns in the vicinity of the heater rod to measure the heat transfer coefficients corresponding to the flow patterns. The latter makes this aim to be attained. On the contrary, this annular flow tube type has the defect that the outer tube wall is apt to be wet with coolant and then, the coolant climbs the wall independently of the flow conditions in the vicinity of the heater rod. But, in so far as the problem is confined to the film boiling region, the characteristics of the film boiling heat transfer depends on whether the

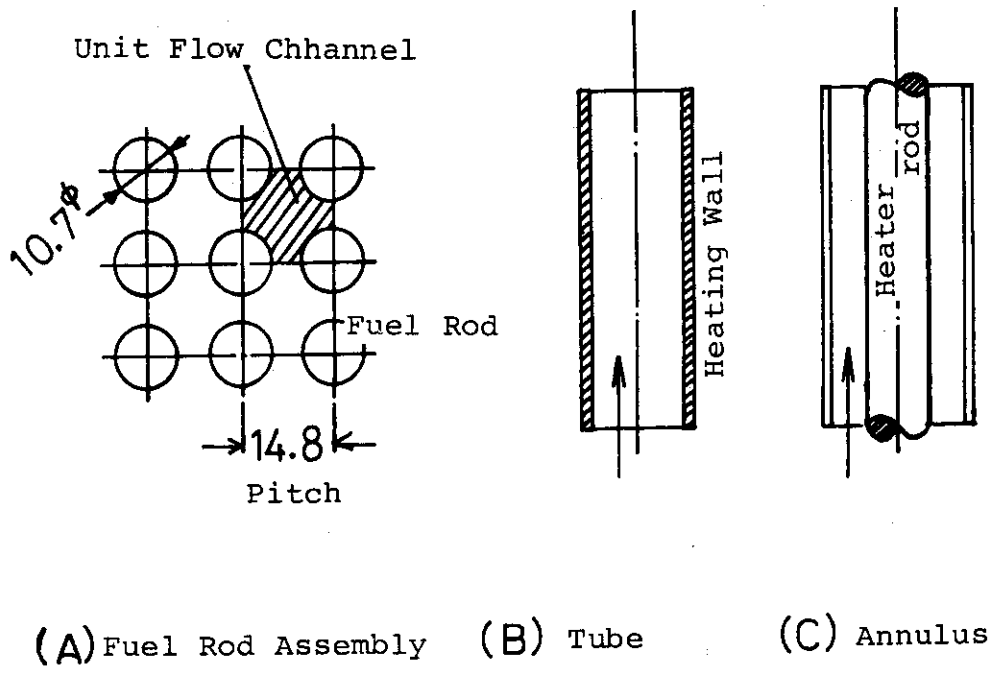

Fig.13 Flow Channel for Experiment

heater rod surface is wet with water or not under the condition that the water exists in the circumference of the high temperature heater rod. Then, the effect that there exists the wall wet with water becomes rather smaller though the length of the film boiling region, the heater rod temperature and so on become different from the situations in the actual core.

By the way, when the electrical power is supplied to the heater rod of the annular flow type, the temperature of the outer tube wall becomes high before the water is injected. Then, the injected water begins to boil on the outer wall when the water is supplied into the flow tube. In this situation, the flow patterns is hard to be observed and is complicated.

In this experiment, the thermal insulation glass tube is set outside the flow tube to avoid this situation.

6. Experimental Results

6.1 The Characteristics of Heater Rod Temperature Histories

Fig. 14 shows the examples of the heater rod temperature histories which are recorded at the elevations 25, 40, 45 cm. The temperature histories which are obtained from the responses of the thermocouples equipped on the heater rod are in general considered to be divided into four stages.

The first stage is the period before the heater rod temperature reaches the maximum, that is, the turnaround Point P. The second stage is the period when the heater rod temperature is falling rather slowly from the turnaround point to the quench point Q. The time when the heater rod temperature begins to fall slowly corresponds to the time when the top level of water reaches where the thermocouple is equipped and that, is the time the level where thermocouple is equipped begins to enter the film boiling region.

The third stage is the period the heater rod temperature falls steeply to the saturation temperature. The point where the rod temperature begins to fall steeply is the quench point. The fourth stage is the period the temperature falls slowly from the saturation temperature to the injected water temperature T_{in}. In Fig. 14, each stage from the first to the fourth is designated as O, A, B and C.

In the 2nd period, the heater rod temperature is above about 300°C and is the temperature at which the heater surface can not be in contact or not be wet with water judging from the thermodynamics. When the water exists in the circumference of the heater rod in this period, the vapour film exists between the water and the heater rod.

Then, it is considered that the heat is transfered under the film boiling. As the heater rod temperature falls steeply to the saturation temperature after the quench, the water can be in contact with heater rod and the nucleate boiling occurs on the heater rod surface. The quench point is approximately considered to be the initiation of the film boiling region as described already.

(1) Effect of the elevations of the rod: The effect of the elevations of the heater rod on the temperature histories is illustrated in Fig. 14. The higher the elevations become, the longer the period A in which the film boiling heat transfer continues and at the same time, the temperature decreases more slowly in this region. And that, even if the heater rod

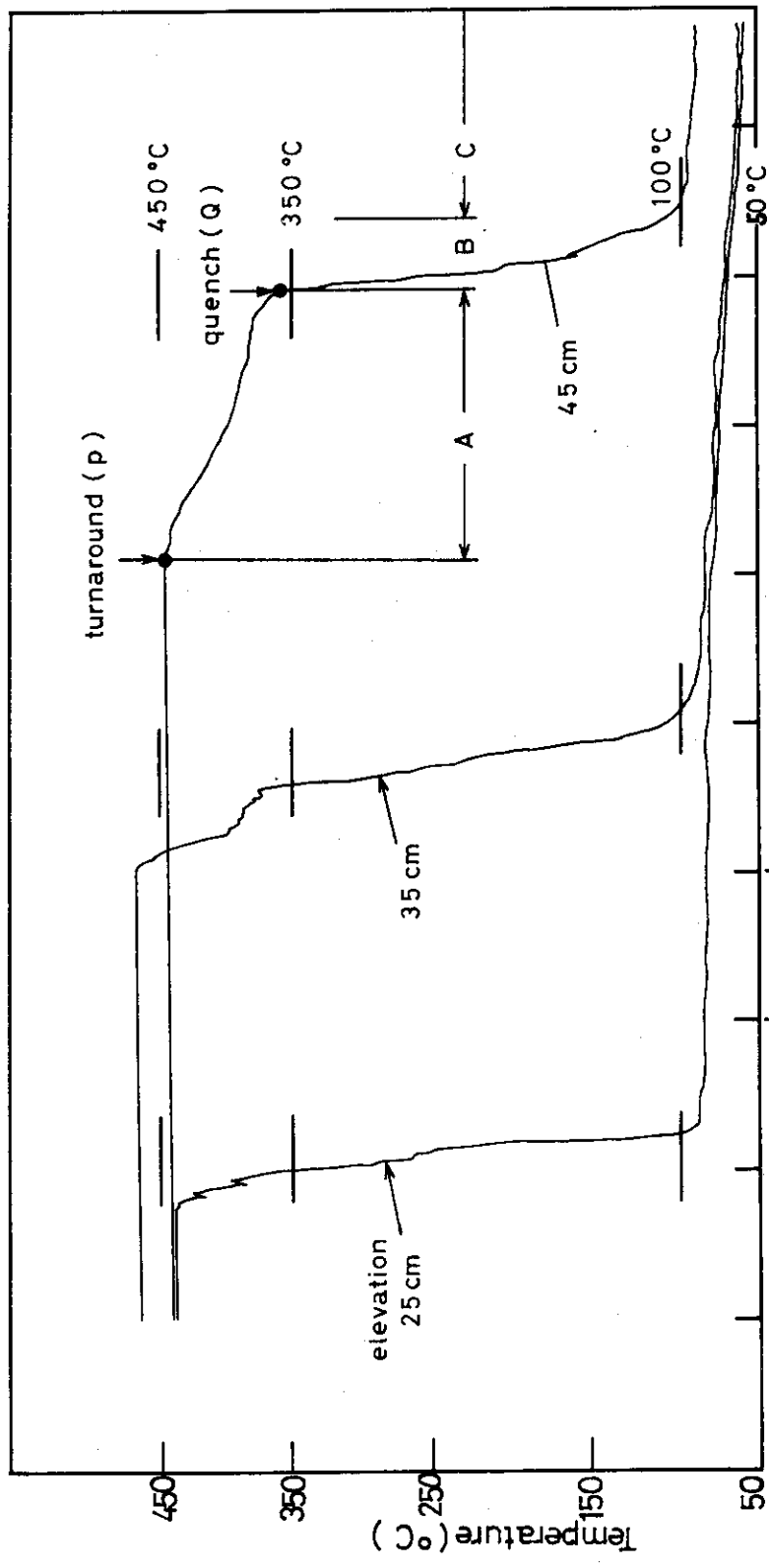

Fig.14 Heater Rod Temperature Profile ; Effects of the Elevatoins in the Single Rod Experiment
($T_{w,int}$=450°C, U_{in}=4.34cm/sec, T_{in}=80°C, P=1 ata)

temperature at the elevation is higher than 400°C the quench occurs just after the level of the water reaches the elevation when the elevation is low and the film boiling region does not at all appear. It is noticed that the condition for the film boiling to appear is not decided only by the rod temperature.

(2) Effect of the initial heater rod temperature: In Fig. 15 is shown the length of the period A, in which the film boiling heat transfer region continues. The elevations illustrated are all 45 cm. The range of the water velocities is from 3.3 to 5.0 cm/s. It is difficult to consider for No.1 and No.2 thermocouple responses to have the film boiling regions because their temperatures are bellow 300°C though the same characteristics as the period A that appears in No.5 thermocouple appear in a short term in them. The periods A in thermocouples No.3, 4 and 5 is considered to be the film boiling region because the temperatures in the periods are above 300°C and because the characteristics is observed that the higher initial rod temperature gives the longer period A and the slower temperature fall in these terms. When the initial temperature becomes above 400°C, the period A which is the film boiling region becomes abruptly longer.

6.2 Relation between the Temperature History and the Flow Pattern Obtained by Photograph

In Fig. 16, is shown a series of photographs which are taken at some internals about the flow patterns in the vicinity of the heater rod. The run conditions are as follows.

inlet water velocity = 1.8 cm/sec
inlet water temperature = 80 °C
initial rod temperature = 600 °C
heat input = 3.8×10^4 kcal/m^2hr
flow tube inner diameter = 22 mm

A scale graduated in millimeter is set along the heater rod. The effective heater section is the part above from 188 mm in the scale. The photographs (1) ∿ (5) show the flow patterns each at the time 3.7, 11.2, 17.0, 21.4 and 29.2 seconds after the water level arrives the start of the effective heater section.

Photograph (1); In the vicinity of the heater rod, the layer of vapour bubbles is formed and the very small vapour bubbles are observed even

NO	Uin	Tw,initial
1	4.6	160
2	3.3	260
3	5.0	360
4	5.0	390
5	4.3	450
	(cm/s)	(°C)

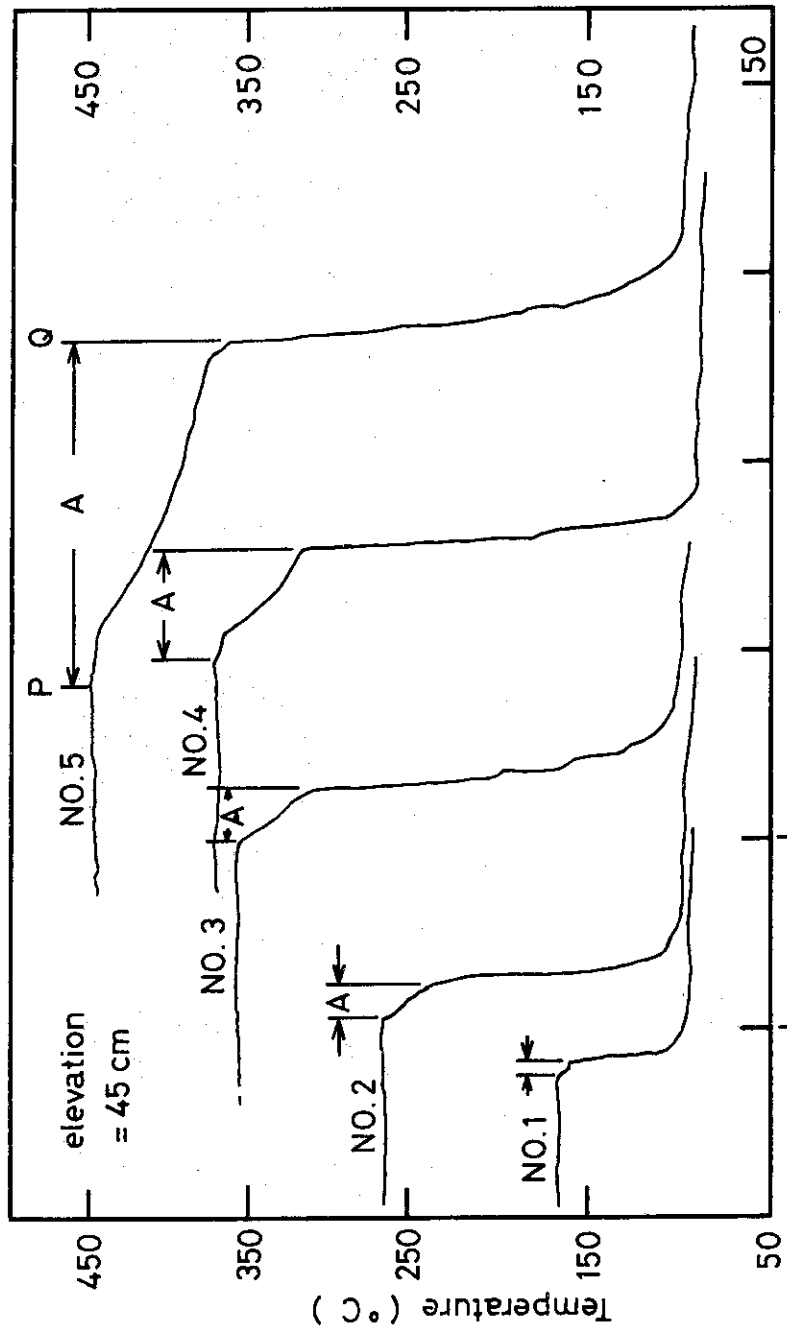

Fig.15 Effects of the Initial Heater Rod Temperatures in the Single Rod Experiment
(T_{in}=80°C, P=1 ata, q=2.5x10^4 kcal/m^{2}hr)

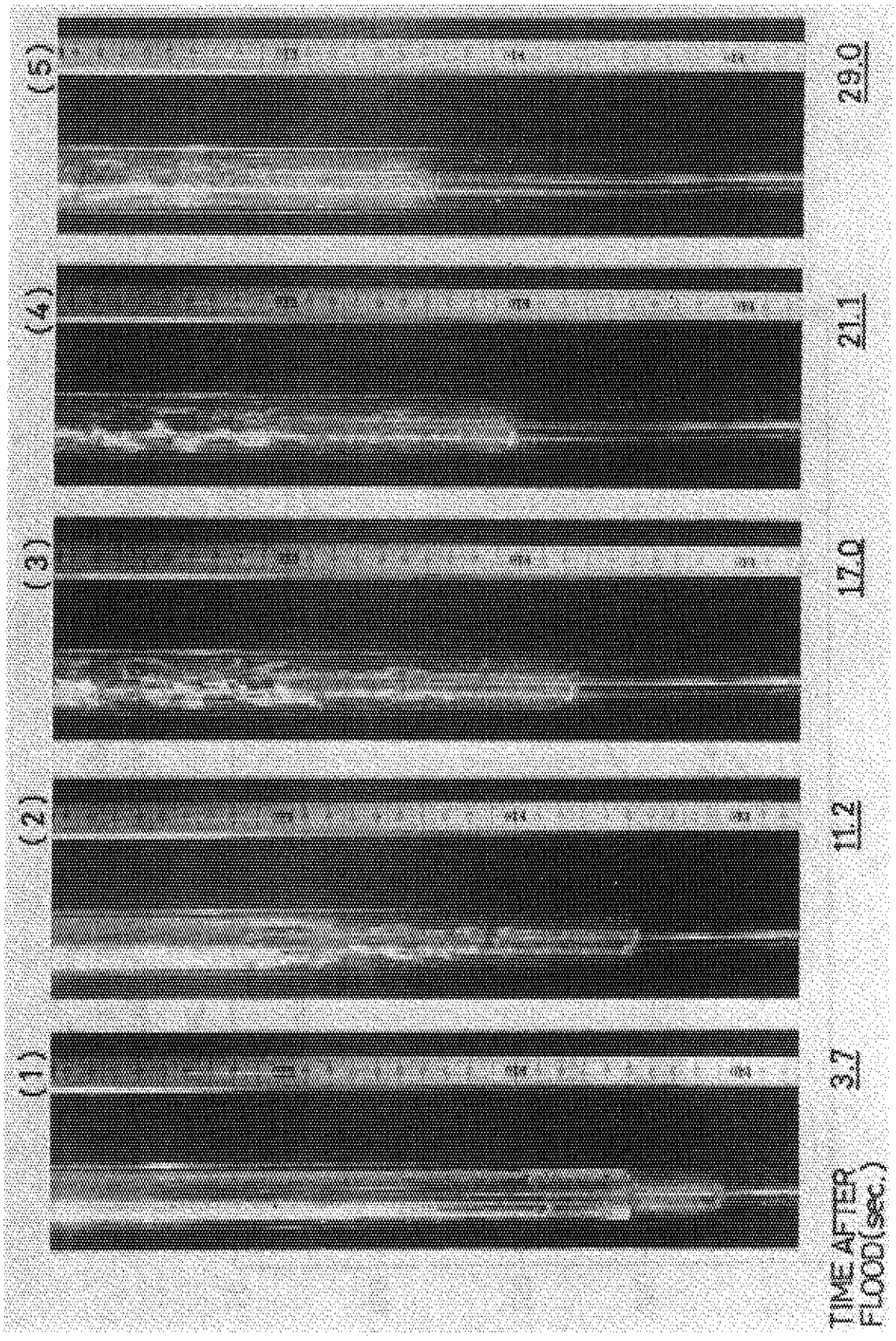

Fig.16 A Series of the Photographs Taken at Intervals during Reflood in the Single Rod Experiment
(T_{in}=80°C, P=1 ata, $T_{w,int}$=600°C, U_{in}=1.8 cm/sec)

in the water in the circumference of the vapour bubbles layer. The water is got muddy in white. The lower end of this vapour bubbles layer is observed definitely. Below this lower end, the heat transfer is done by forced convection as the rod temperatue is bellow 100°C and above this end it is done by nucleate boiling as the rod temperature is above 100°C at most by 10°C. By this time the film boiling does not occur. When the top level of water reaches the some elevation, the rod temperature falls suddenly near to the saturation temperature.

Photograph (2); Along the heater rod, a rather complicated flow pattern is observed. In the lowerest part of the heater rod the forced convection heat transfer region exists where the heater rod is observed clearly. In the vicinity of the heater rod above this region the vapour bubbles layer is observed and the nucleate boiling occurs there. Above the nucleate boiling region, the film boiling region exists, where vapour film is recognized in the circumference of the heater rod. In this region the heater rod temperature is above 300°C. With this temperature the water can not be in contact directly with the surface of the heater rod under the stable state. Above this film boiling region the water level is turbulent and the boundary of the water and the vapour is rather apart from the heater rod surface. The top level of water can't be decided definitely as the flow patterns is complicated. On the other hand, the quench point is not determined by the photograph and is determined only by the temperature responses.

Photographs (3), (4), (5); As the time elapses, the flow patterns move from the photograph (3) to photograph (5) and each heat transfer region becomes longer. Especially in the photograph (3) rather definite existance of the vapour film is recognized in the vicinity of the rod between 350 mm and 420 mm on the scale. This region is the film boiling. As the time elapses, the top level of water becomes more turbulent and the larger lumps of water are scattered upwards.

6.3 Film Boiling Heat Transfer Coefficients

The characteristics of the film boiling heat transfer coefficients h_c are investigated with the relation of h_c and the length L (representative length) from the elevation where the thermocouple is equipped to the quench point bellow. The calculations of the heat flux and the local subcooling at each elevation are shown in Appendices A and B

6.3.1 The effect of the elevations of the heater rod; At each elevation the characteristics of the heat transfer coefficients histories are different even under the same run because the local subcooling of water becomes smaller along the heater rod. In Fig. 17, the heat transfer coefficients h_c at the elevations 20, 45, 70 cm are illustrated with selecting the length L as the ordinate and h_c as the abscissa. The run conditions are shown in the figure. In the film boiling region, the lower elevation shows the higher heat transfer coefficients with the same length L. At the elevation 70 cm the local subcooling is zero, that is, the water temperature is saturation temperature from the calculation of the local subcooling. The effect of the elevation on h_c can be said to be the effect of the local subcooling judging from the fact that the local subcooling diminishes along the heater rod.

6.3.2 Saturated film boiling heat transfer coefficients $h_{c,sat}$;

Even if the subcooled water is supplied into the flow tube, the water can become the saturation temperature T_s at some elevations because the water receives the heat input from the heater rod and the water temperature rises along the heater rod to the saturation temperature, when the saturated film boiling occurs. In Fig. 18, is illustrated the saturated film boiling heat transfer coefficients $h_{c,sat}$ with respect to the representative length L. In the figure the ordinate shows the length L and the abscissa shows the convective heat transfer coefficients $h_{c,sat}$, which is obtained as follows.

$$h_t = h_c(h_c/h_t)^{1/3} + h_r \tag{11}$$

$$h_r = 4.88 \left\{\left(\frac{T_w}{100}\right)^4 - \left(\frac{T_s}{100}\right)^4\right\}/(T_w - T_s) \quad \left[\frac{\text{kcal}}{\text{m}^2\text{hr°C}}\right] \tag{12}$$

where h_t is the total coefficient and h_r is the radiative coefficient. Whether the local temperature of water has become the saturation temperature at some elevation is judged from the Eqn. (B-6) in Appendix B. The representative length L is calculated from Eqns. (1) and (2). Run conditions are shown in the figure.

As seen in the figure, the following characteristics are pointed out of the saturated film boiling heat transfer.

(1°) With the same length L, the coefficients $h_{c,sat}$ are approximately the same although the inlet temperature and velocity of water are different.

$T_{w,int}$=600°C, T_{in}=80°C, U_{in}=1.8cm/sec.				
Symbol	○	△	●	
Elevation	70	40	20	(cm)

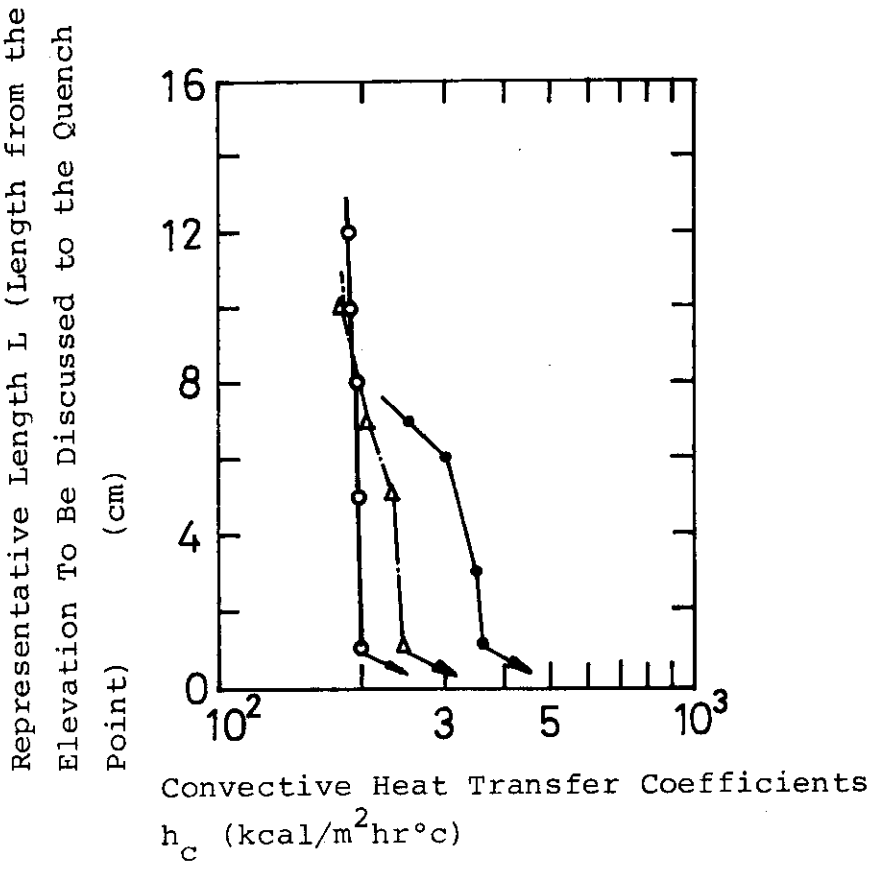

Fig.17 Effects of Elevations on Convective Heat Transfer Coefficients h_c in Single Rod Experiment

SYMBOL	▽	ⓓ	✦	○	unit
ELEVATION	40	40	40	70	cm
INJECTED WATER TEMPERATURE	97	97	97	80	°C
INJECTED VELOCITY	4.0	2.5	2.5	1.8	cm/sec
ELECTRIC POWER	(2.4-5.0)x10000				kcal/m^{2}hr
INITIAL CLAD TEMPERATURE	625			600	°C

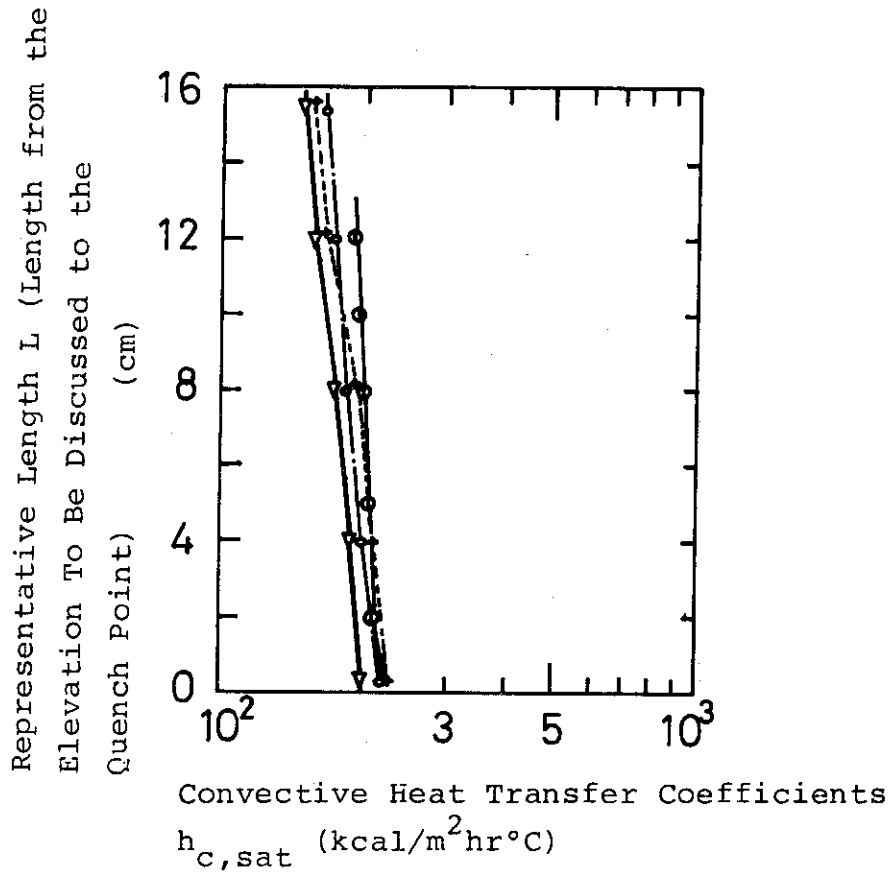

Fig.18 Saturated Film Boiling Heat Transfer Coefficients $h_{c,sat}$ with Respect to the Representative Length L in Single Rod Experiment

(2°) The tendency is clearly observed that $h_{c,sat}$ becomes smaller as the length L becomes longer.

6.3.3 Subcooled film boiling heat transfer coefficients $h_{c,sub}$;

The results of the relations between h_c and the length L are shown in Fig. 19, which are investigated with respect to the inlet water subcooling. Group number 1 shows the results of inlet water subcooling 3°C, Group number 2 shows the ones of 10°C, Group number 3 shows the ones of 20°C and Group number 4 shows the ones of 60°C. In the same group number, the water velocity is different in each run. The elevation is 40 cm and is all the same. From Fig. 19, the following characteristics are recognized.

(i) The larger inlet water subcooling gives the larger heat transfer coefficients h_c with the same length L.

(ii) Under the same inlet water subcooling the heat transfer coefficients h_c become larger with the same length L when the water velocity is larger.

The result in Group number 1 shows the saturated film boiling heat transfer coefficients $h_{c,sat}$ because at the elevation 40 cm the water temperature has become the saturation temperature by the heat input from the heater rod. This is shown for comparison.

In the results in other Group numbers, it may be considered that the subcooled film boiling heat transfer occurs at the elevation 40 cm because the water temperature at the elevation is bellow the saturation temperature.

Group No.	Symbol	Quench Velocity (cm/s)	T_{in} (°C)	U_{in} (cm/s)
1	○	0.8-0.9	97	2.5
	◎			4.0
	□			5.5
2	▼	1.0	90	2.5
	▲			5.7
3	⊕	1.0	80	2.0
	⊙			2.5
	✦	2.2		6.0
4	○	3.0	40	4.2

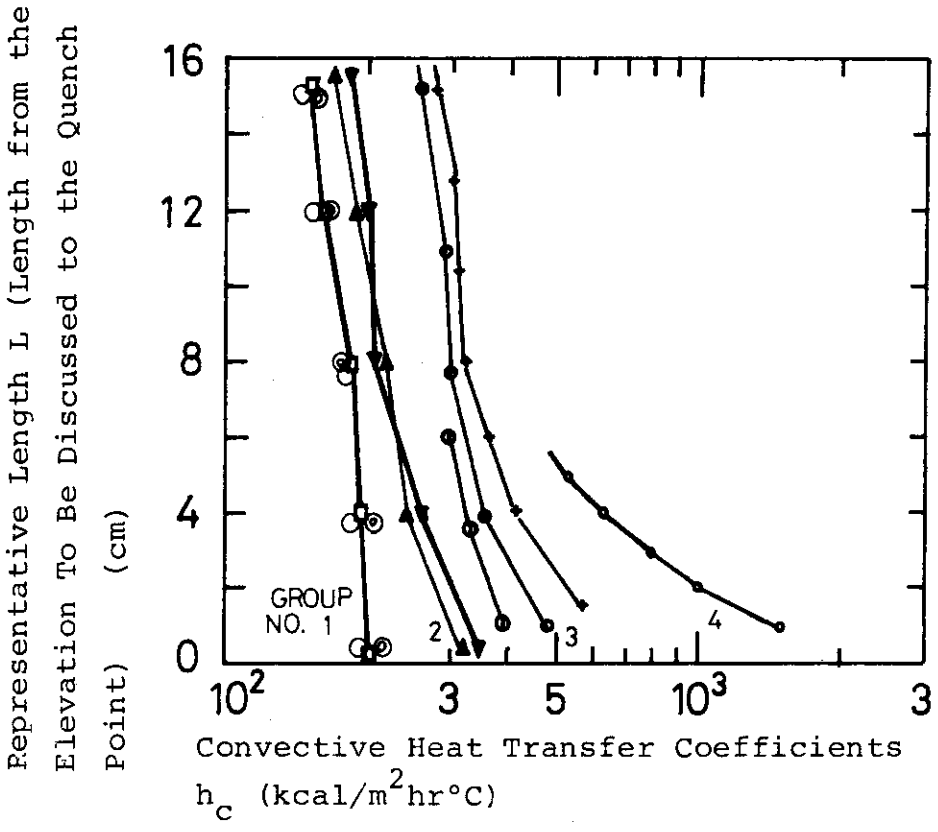

Fig.19 Subcooled Film Boiling Heat Transfer Coefficients $h_{c,sub}$ in the Single Rod Experiment

7. Analysis and the Discussion of the Experimental Results

From the preliminary analysis for the PWR FLECHT TEST data and the experiment for the film boiling heat transfer, the followings are made clear.

(i) When the water temperature becomes the saturation temperature at some elevations, the characteristics of h_c with respect to the representative length L take the same tendencies at these elevations even if the subcooled water is supplied into the test section (heat transfer coefficients are almost the same with the same length L).

(ii) When the water velocity is small, the water subcooling at the elevation to be discussed can become small or to be zero even if the inlet water subcooling is very large.

(iii) Then, to discuss the effect of the water subcooling on h_c, it is necessary to investigate the local subcooling.

In this chapter, the saturated heat transfer coefficients $h_{c,sat}$ are first evaluated quentitatively and then, the subcooled ones $h_{c,sub}$ are evaluated with using the subcooling ΔT_{sub} and $h_{c,sat}$.

7.1 Saturated Heat Transfer Coefficients $h_{c,sat}$

7.1.1 Applicability of the previous studies' results;

(i) Berenson Correlation[5]

In the U.S. loss-of-coolant code RELAP4, the Berenson correlation is used for a stagnation condition.

$$h = 0.425 \left[\frac{k_v^3 g_c \rho_v (\rho_L - \rho_v) h_{fg}'}{\mu_v \Delta T (\frac{\lambda_c}{2\pi})}\right]^{1/4} \tag{13}$$

This correlation is derived for film boiling on a horizontal flat plate. The thin vapour film over the horizontal surface is unstable and large bubbles are formed and break away. The characteristic spacing of these bubbles λ_c is determined by

$$\frac{\lambda_c}{2\pi} = \left[\frac{\sigma}{g(\rho_L - \rho_v)}\right]^{1/2} \tag{14}$$

This correlation is compared with the FLECHT TEST results in Fig. 20.

(ii) Bailey correlation[14]

Bailey suggested that the globular voids are formed on vertical heated

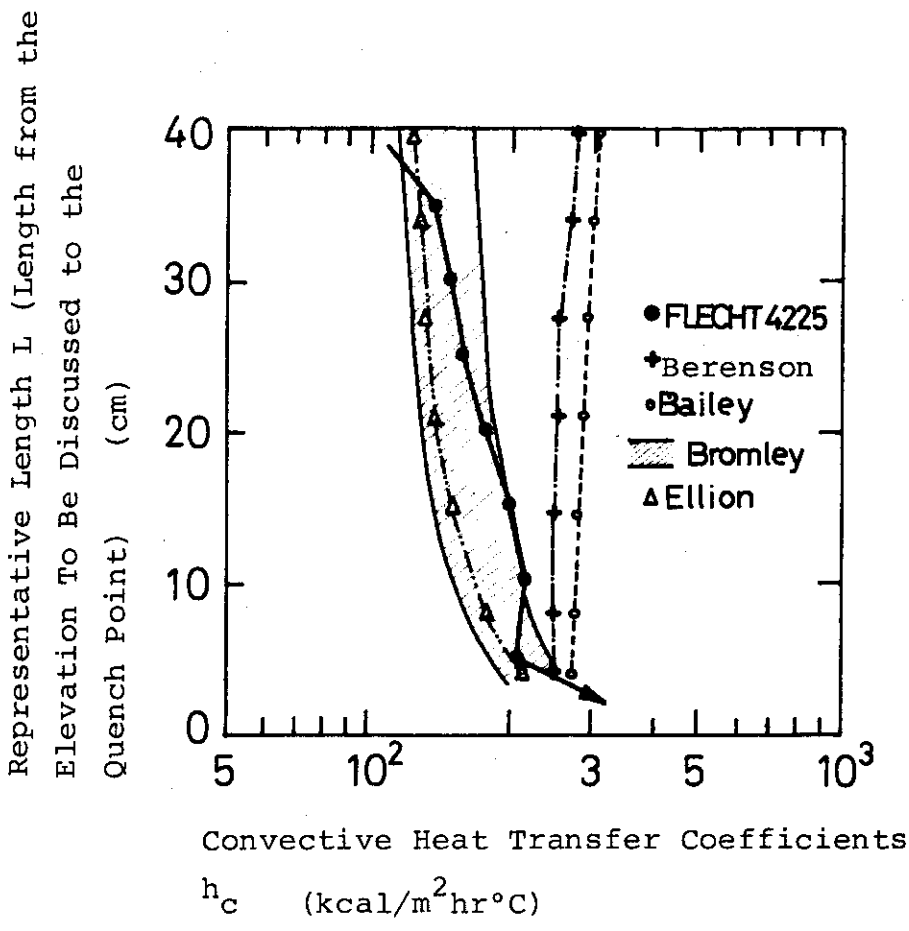

Fig.20 Comparison of the Previous Film Boiling Correlations (Berenson, Bailey, Bromley and Ellion) with PWR FLECHT Test

surfaces by a process of varicose instability of a hollow gas cylinder within a denser liquid as proposed by Chandrasekhar. He proposed the correlation,

$$h = \left[\frac{k_v^3 g_c \rho_v (\rho_L - \rho_v) h_{fg}'}{4\mu_v \Delta T (\frac{\lambda_c}{2\pi})}\right]^{1/4} \tag{15}$$

$$\frac{\lambda_c}{2\pi} = \frac{\frac{1}{2} d}{0.484} \tag{16}$$

where d is the fuel rod diameter.

This correlation is also compared with the FLECHT TEST results in Fig. 20.

(iii) Bromley correlation[8] and Ellion correlation[2]

In addition to developing the theory for film boiling on horizontal cylinders, Bromley also gave the results of the same type of theoretical treatment for a vertical tube or plate.

$$h = c \left[\frac{k_v^3 g_c \rho_v (\rho_L - \rho_v) h_{fg}'}{L\mu_v \Delta T}\right]^{1/4} \tag{17}$$

The value of the constant c in this case is between 0.667 and 0.943.

Bromley did not represent experimental data to check the validity of the result; however Ellion[2] later developed a similar theoretical result,

$$h_c = 0.714 \left[\frac{k_v^3 g_c \rho_v \rho_L h_{fg}'}{L\mu_v \Delta T}\right]^{1/4} \tag{18}$$

and represented some experimental data to substantiate this equation. These correlations are compared with the FLECHT TEST data in Fig. 20.

(iv) Grietzer and Abernathy's study[15]

Another recent study of vertical film boiling was done by Greitzer and Abermathy. They considered that the large vapour bubbles released from the film and took account of the time-varying vapour thickness. This study also indicates that the smooth interface laminar flow solution, equation (17) predicts a value of approximately two too low. The effects of subcooling and liquid velocity are also established for methanol over a wide range of values. Typically increasing the liquid velocity from 0 to 15 ft/sec or alternatively the subcooling from 0 to 45°F might double the heat transfer coefficients in each case.

7.1.2 Evaluation of $h_{c,sat}$;

As one of the characteristics of the film boiling heat transfer during reflood, it is pointed out that heater rod surface temperature is not uniform but has the distribution along the rod from the start of the film boiling to the portion to be discussed. Then, to evaluate the local heat transfer coefficients at the portion to be discussed it is necessary to consider the temperature profile from quench point to that portion.

From the same treatment as done by Bromley, the vapour film thickness a_v is expressed as follows at the arbitrary elevation L.

$$a_v^4 = \int_0^L C \frac{\mu_v}{\gamma_v \gamma_L} \frac{k_v(T_w - T_s)}{h_{fg}'} dZ \tag{19}$$

For simplicity, the temperature profile T_w between the quench (Z = 0) and the elevation (Z = L) is expressed as

$$T_w = (T_{w(Z=L)} - T_Q)Z/L + T_Q \tag{20}$$

As vapour temperature used to evaluate the physical properties such as μ_v, k_v and so on, the following average temperature is used.

$$\bar{T}_G = 0.5[0.5(T_{w(Z=L)} + T_w) + T_s] \tag{21}$$

Then, a_v is approximately evaluated as follows at Z = L.

$$a^4_{v_{Z=L}} = c \left[\frac{\mu_v k_v}{h_{fg}' \gamma_v \gamma_L} \right]_{\bar{T}_G} \left(\frac{T_{w(Z=L)} + T_Q}{2} - T_s \right) \tag{22}$$

$$h_{c,sat}\Big|_{Z=L} = \frac{k_{v(Z=L)}}{a_{v(Z=L)}} \tag{23}$$

$$= C_o \cdot k_{v_{T_{G(Z=L)}}} \cdot \left[\frac{\gamma_v \gamma_L h_{fg}'}{L \mu_v k_v \left(\frac{T_{w(Z=L)} + T_Q}{2} - T_s \right)} \right]^{1/4}_{\bar{T}_G} \tag{24}$$

where $\bar{T}_G = 0.5[0.5(T_{w(Z=L)} + T_Q) + T_s]$

$$T_{G(Z=L)} = 0.5(T_{w(Z=L)} + T_s) \tag{25}$$

$$C_o = C^{-1/4}$$

In equation (24), the value of constant C_o is not yet determined. Although this value is theoretically determined from the vapour velocity profile across the vapour film, it involves the uncertainty of the validity of this analysis. Then, it is tried conversely to determine the value C_o by comparing with experimental results. The values C_o determined with the experimental results $(h_{c,sat})_{experiment}$ can be expressed as

$$C_o = \frac{(h_{c,sat})_{experiment}}{\frac{k_v}{T_{G(Z=L)}} \cdot \left[\frac{\gamma_v \gamma_L h_{fg}'}{L\mu_v k_v \left(\frac{T_{w(Z=L)}+T_Q}{2} - T_s\right)_{\bar{T}_G}}\right]^{1/4}} \qquad (26)$$

The results are shown in Fig.21(A) by taking C_o as the ordinate and the length L as the abscissa. The results obtained from the PWR FLECHT test data are shown in Fig. 21(B). Although the values of constant C_o are dependent of the length L, the bold line $C_o = 0.94$ expresses the characteristics of the values C_o fairly accurately. This value $C_o = 0.94$ is near the value (0.943) introduced in Bromley's analysis under the boundary condition of zero interfacial shear stresses.

7.2 Subcooled Heat Transfer Coefficients $h_{c,sub}$

Although it is well known that the subcooled film boiling heat transfer coefficients $h_{c,sub}$ become larger than the saturated ones $h_{c,sat}$, the valid evaluation for $h_{c,sub}$ has not yet been carried out and that, it is not made clear quantitatively how much the coefficients increase compared to the saturated film boiling heat transfer coefficients when the subcooling exists. Then, as one of the means to evaluate the effect of the subcooling, the ratios of $h_{c,sub}$ to $h_{c,sat}$ are investigated with regard to the subcooling in Fig. 22.

In this figure, the ordinate shows the ratio $h_{c,sub}/h_{c,sat}$, the absissa shows the subcooling and the heater rod surface temperatures are also shown as the parameter. The FLECHT test results are expressed with the - marks. The results of this experiment are expressed with - marks. The values $h_{c,sat}$ in the ratios $h_{c,sub}/h_{c,sat}$ are evaluated from eqns. (24) and (26) and the values $h_{c,sub}$ are experimental results. From this figure the followings are pointed out.

(i) The ratios $h_{c,sub}/h_{c,sat}$ become large in general in each run in proportion to the increases of subcooling though they have the some range of fluctuation.

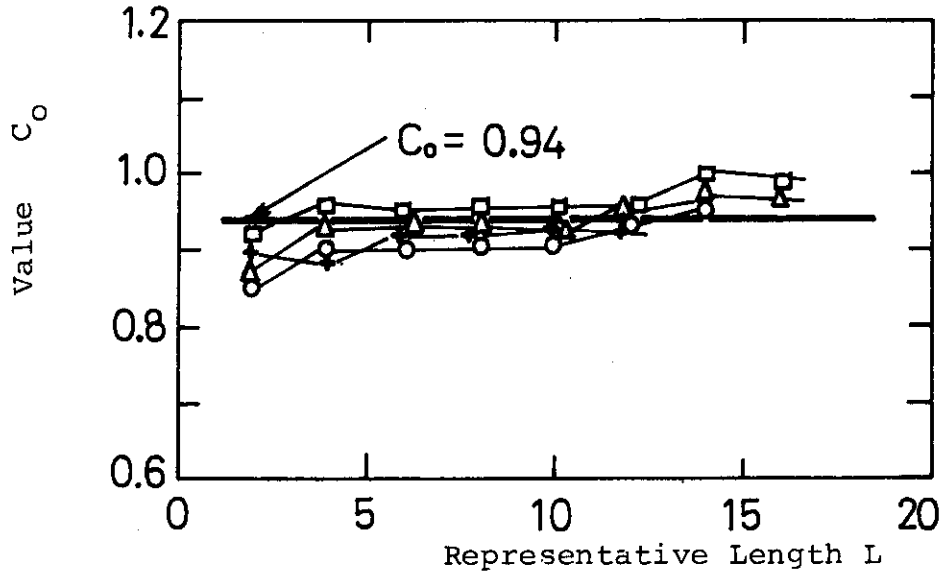

(A)Single Rod Experiment

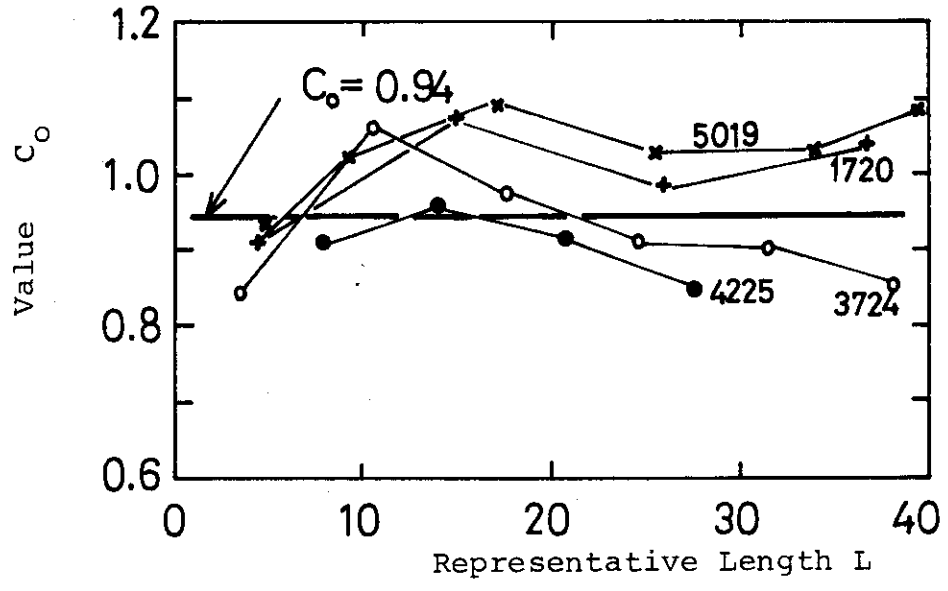

(B)FLECHT TEST Data

Fig.21 Determination of the Constant Value C_o with the Experimental Results on the Saturated Film Boiling Heat Transfer Coefficients $h_{c,sat}$

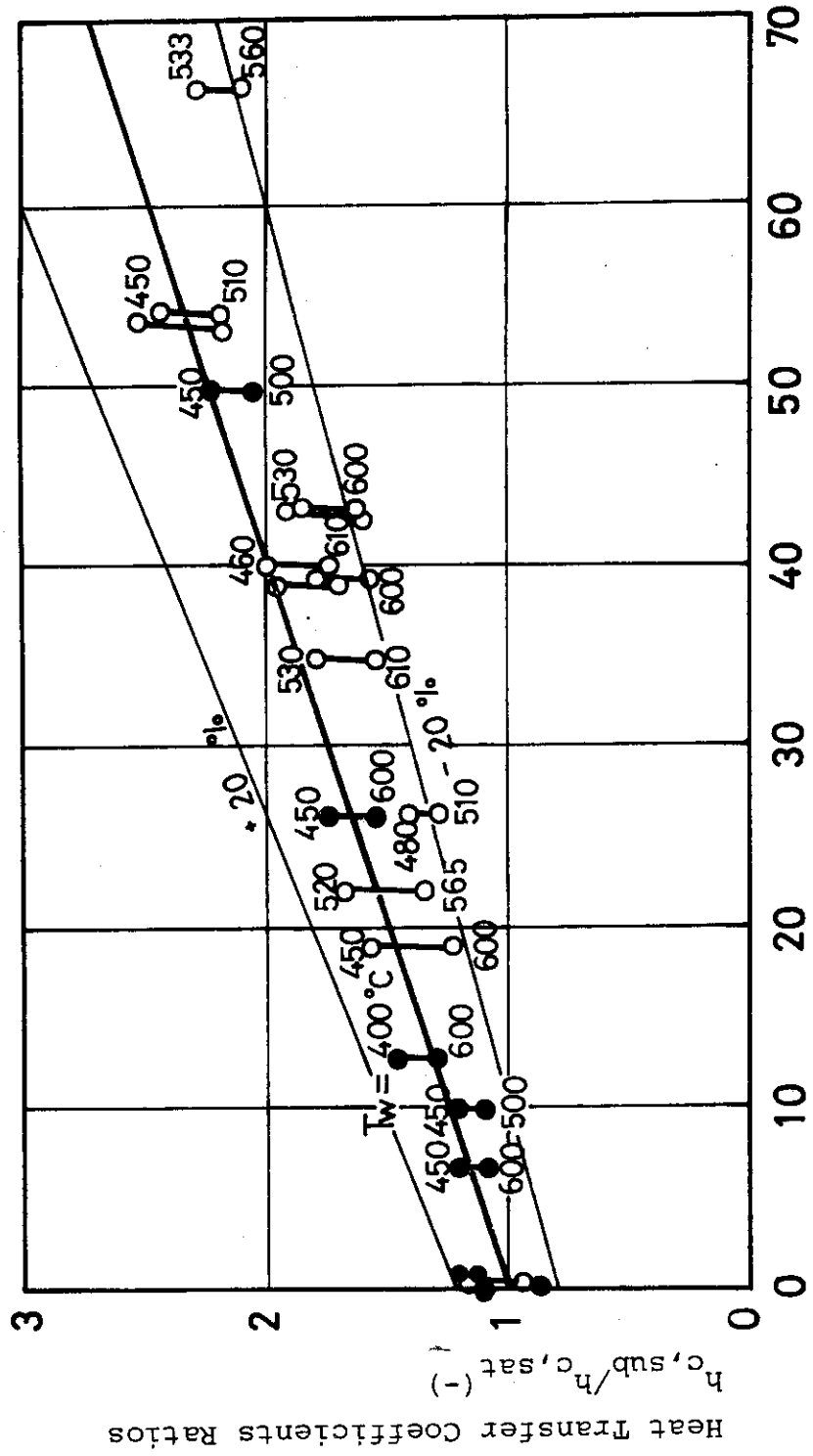

Fig.22 Relation between the Ratios $h_{c,sub}/h_{c,sat}$ and the Subcooling T_{sub}; Summary of Effects of the Subcooling on Heat Transfer Coefficients

(ii) Each run has the common tendency that the ratios become larger when the surface temperature are low than when they are high. That the surface temperature are high inplies that the quench point, that is, the start of the film boiling is far bellow the elevation to be discussed and that the length L is large. On the other hand, that the surface temperature is low implies contradictory condition in general.

(iii) Although the data are scattering in rather broad range, the characteristics of $h_{c,sub}$ with repeat to the local subcooling ΔT_{sub} can be grasped with the bold line in the figure. The error the bold line represents is within ±20 %. Then, the subcooled film boiling heat transfer coefficients $h_{c,sub}$ are evaluated with the accuracy within ±20 % error as follows.

$$h_{c,sub} = (1 + 0.025 \quad T_{sub})h_{c,sat} \tag{27}$$

$$h_{c,sat} = 0.94 \cdot k_{v\,(Z=L)} \cdot \left[\frac{\gamma_v \gamma_L h_{fg}'}{L\mu_v k_v \left(\frac{T_{w(Z=L)}+T_Q}{2} - T_s\right) \bar{T}_G}\right]^{1/4} \tag{28}$$

where ΔT_{sub} is the subcooling in degree C, $\bar{T}_G$ is 0.5 $(0.5(T_{w(Z=L)} + T_G) + T_s)$ and the physical properties in the bracket [ ] are evaluated with the temperature $\bar{T}_G$.

7.3 Limitation on the Applicability of the Relation between $h_{c,sub}/h_{c,sat}$ and ΔT_{sub}

It is impossible to read the film boiling heat transfer coefficients in the vicinity of the quench point (in the region 0 ∿ 5 cm above the quench point) in the PWR FLECHT test data sheets. Furthermore, it can not be considered as reasonable that the value which is obtained without taking into account the heat conduction along the heater rod in the vicinity of the quench point, is the true film boiling heat transfer coefficients just above the quench point. As the uncertainties are left in the vicinity of the quench point as described above, the applicability of the relation between $h_{c,sub}/h_{c,sat}$ and ΔT_{sub} is restricted in the region except for the vicinity of the quench point, to say concretely, in the length larger than 5 cm above the quench point.

8. Conclusion

To make clear the characteristics of the film boiling heat transfer during the reflood and to evaluate the heat transfer coefficients, the investigation on the PWR FLECHT test data and single rod film boiling test were carried out. As the results, the followings were made clear.

(1) By considering the representative length L which is defined as the one from the quench point to the upper elevation to be discussed, the effects of injected water velocity, inlet water temperature, initial rod temperature and system pressure on heat transfer coefficients are made clear. Under the same conditions of other parameters, the heat transfer coefficients h_c become larger as the inlet subcooling and injected water velocity become larger. Initial rod temperature does not make effect on h_c significantly.

(2) The local subcooling was determined from the inlet water subcooling, the injected water velocity and heat release from the heater rod. This subcooling was found to make a great effect on h_c.

(3) As the start of the film boiling during the reflood the quench point can be taken. By the length L from this point to the elevation to be discussed, the effect of the elevation on h_c can be evaluated approximately.

(4) The saturated film boiling heat transfer coefficients $h_{c,sat}$ can be evaluated well with the same type as the Bromley's correlation by selecting 0.94 as the value of the constant C_o. The expression is as follows.

$$h_{c,sat} = 0.94\ k_{v\,(Z=L)} \left[\frac{\gamma_v \gamma_L h_{fg}'}{L\mu_v k_v \left\{\frac{T_{w(Z=L)}+T_Q}{2} - T_s\right\} \bar{T}_G}\right]^{1/4}$$

(5) The subcooled film boiling heat transfer coefficients $h_{c,sub}$ can be evaluated as follows with the local subcooling ΔT_{sub} and the saturated film boiling heat transfer coefficients $h_{c,sat}$ with the accuracy less than ±20 % error.

$$h_{c,sub} = (1 + 0.025\ T_{sub}) h_{c,sat}.$$

Acknowledgement

The authors are grateful to Y. Yamazaki, ex-deputy head of division of reactor safety, to Dr. M. Nozawa, deputy head of division of reactor safety and to Dr. K. Hirano, reactor safety lab. II chief for much helps during this study. Grateful appreciation is also expressed to Y. Fukaya and Y. Niitsuma for much advices and helps in the experiment.

Appendix A

Calculation of heat flux from the rod surface;

As the heater rod temperature is varying with time, heat release of the stored energy in the rod must be taken into account as the heat flux as well as the heat generation by electric power supply. It is not valid to consider that temperature across the cross section of the rod is uniform and that it falls at constant rate with time.

Under the following assumptions that will be reasonable in the film boiling region with respect to the temperature profile, the heat flux is obtained (see Fig. A-1).

(i) The temperature along the rod in the film boiling region is uniform as the temperature change is rather moderate there. The quench region where temperature changes steeply is not considered here.

(ii) The temperature across the cross section of the rod is expressed as

$$T(r,t) = A(t)\cdot r^2+B(t)\cdot r + C(t) \tag{A-1}$$

A(t),B(t) and C(t) are the coefficients dependent on time t.

$$\frac{k}{r}\frac{\partial}{\partial r}\left(r\frac{\partial T(r,t)}{\partial r}\right) + g_o = C_p\frac{\partial T(r,t)}{\partial t} \qquad R_0 < r < R_1 \tag{A-2}$$

boundary conditions

$$\text{(a)}\quad \left.\frac{\partial T(r,t)}{\partial r}\right|_{r=R_0} = 0 \tag{A-3}$$

$$\text{(b)}\quad \left.T(r,t)\right|_{r=R_1} = F(t) = T_0(1-at) \tag{A-4}$$

$$\text{(c)}\quad T = T_1 \quad \text{at } r = R_0,\ t = 0 \tag{A-5}$$

$$\text{(d)}\quad T = T_0 \quad \text{at } r = R_1,\ t = 0 \tag{A-6}$$

$$A(t) = \left(\frac{a_3}{a_2} - \frac{T_1-T_0}{R_1^2-R_0^2}\right)e^{\frac{a_2}{a_1}t} - \frac{a_3}{a_2} \tag{A-7}$$

$$a_1 = \frac{1}{12}\left(SR_0^3 + 17R_0^2R_1 + 11R_0R_1^2 - 9R_1^3\right) \tag{A-8}$$

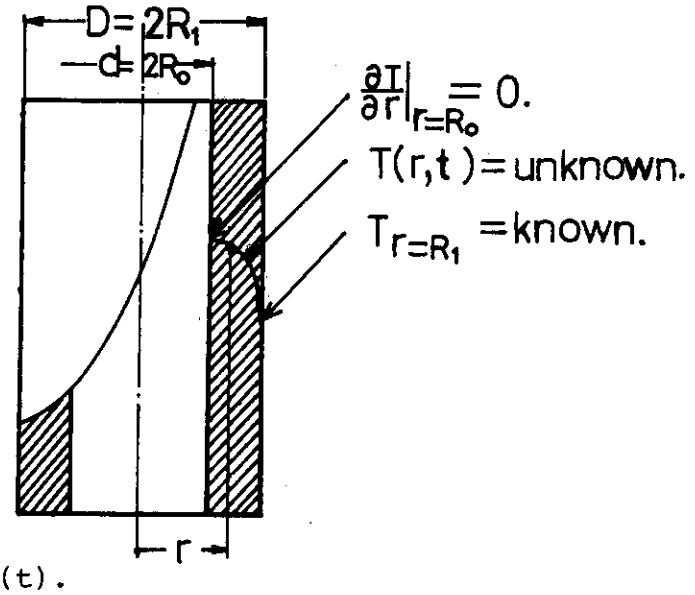

$$T(r,t)= A(t).r^2+B(t).r+C(t).$$

Fig.A-1 Temperature Profile in the Rod Used for Calculating the Heat Flux from the Rod Surface

$$a_2 = \frac{2k}{C_p\gamma} R_1 \tag{A-9}$$

$$a_3 = \frac{R_0+R_1}{2} \left(\frac{g_o}{C_p\gamma} + a\right) \tag{A-10}$$

Then,

$$h = \frac{q}{T_w-T_s} \tag{A-11}$$

$$= \frac{k}{T_w-T_s} \frac{\partial T}{\partial r}\Big|_{r=R_1} \tag{A-12}$$

$$= \frac{2k(R_7-R_0)}{T_w-T_s} \frac{a_3}{a_2} + \left(\frac{T_1-T_0}{R_1^2-R_0^2} - \frac{a_3}{a_2}\right)e^{\frac{a_2}{a_1}t} \tag{A-13}$$

When the temperature history at the outer surface of the rod cannot be approximated to change linearly with time such as $T_0(1-at)$, it is assumed for the temperature to change linearly with time in some time intervals.

Appendix B

The determination of the local subcooling in this single rod experiment;

In the experiment the boiling on the inner surface of the flow tube is avoided because the thermal insulation tube outside the flow tube is filled with water of the same temperature as the inlet water. The temperature of water supplied into the flow tube rises along the heater rod. On the other hand, through the flow tube wall the heat releases. Then the local subcooling is estimated approximately as follows.

With respect to the temperature rise of water flowing upwards with velocity u, the heat balance in the intervals dZ along the rod is

$$(\frac{\pi}{4})(D^2-d^2)\gamma C_p\, dT = \pi d q_1 dZ/u - \pi D q_2 dZ/u \tag{B-1}$$

$$q_2 = \frac{ks}{\delta}(T - T_{\ell o}) \tag{B-2}$$

where D is the diameter of flow tube, d the diameter of rod, γ the specific weight of water, C_p heat capacity of water, T water temperature, u water velocity, q_1 the heat flux from rod, q_2 the heat flux through the flow tube wall, δ the thickness of the flow tube wall, k_s the thermal conductivity of the flow tube wall and $T_{\ell o}$ the water temperature in the thermal insulation tube (constant).

$$u(D^2-d^2)\gamma C_p \frac{dT}{dZ} = 4\{q_1 d - \frac{k_s}{\delta} D(T - T_{\ell o})\} \tag{B-3}$$

As the inlet temperature is given as $T = T_{\ell o}$ at $Z = 0$, the subcooling at $Z = Lo$ is expressed as

$$\Delta T_{sub} = T_s - T_{z=Lo} \tag{B-4}$$

$$= (T_s - T_{\ell o}) - (T_{z=Lo} - T_{\ell o}) \tag{B-5}$$

$$= (T_s - T_{\ell o}) - \frac{\delta d q_1}{D k_s}\left[1 - \exp\left\{-\frac{4 k_s D Lo}{\delta C_p \gamma u (D^2-d^2)}\right\}\right] \tag{B-6}$$

References

(1) WCAP-7435, PWR FLECHT GROUP I TEST REPORT (1972).

(2) M. E. Ellion, A study of the mechanism of boiling heat transfer. Memo 20-88, Jet Propulsion Lab., Pasadena, California, 1954.

(3) L. A. Bromley et al., Heat Transfer in forced convection film boiling. Ind. Eng. Chem. 45, 2619 (1953).

(4) Y. P. Chang, A theoretical analysis of heat transfer in natural convection and in boiling. ASME 71, 1501 (1957).

(5) P. J. Berenson, "Film boiling heat transfer from a horizontal surface". Trans. ASME, Journal of Heat Transfer 83, C. (1961).

(6) N. Zuber, On the stability of boiling heat transfer. Trans. ASME 80, 711 (1958).

(7) R. D. Cess and E. M. Sparrow, Film boiling in a forced-convection boundary-layer flow. F. Heat Transfer 83, p.377 (1961).

(8) L. A. Bromley, Heat transfer in stable film boiling. Ph. D. Thesis, Dep. of Chem., Univ. of Californiа, Berkeley, California, 1948, also, AEC-2295.

(9) Y. Y. Hsu and J. W. Westwater, Film boiling from vertical tubes. A. I. Ch. E. J. 4. p.58 (1958).

(10) F. Tachibana and S. Fukui, Heat transfer in film boiling to subcooled liquids. In "International Developments in Heat Transfer", p.219 Am. Soc. Mech. Eng., New York, 1961.

(11) L. A. Bromley, Heat Transfer in stable film boiling. Chem. Eng. Progr. 46, p.221 (1950).

(12) F. Tachibana et al., Trans. of JSME, Feb. 1970.

(13) K. Ishigai et al., Trans. of JSME, 29, 348, 1963.

(14) N. A. Bailey, "Film boiling on submerged vertical cylinders". AEEW-M1051 (1971).

(15) E. M. Greitzer and F. H. Abernathy, "Film boiling on vertical surfaces". Int. J. Heat Mass Transfer, 15 p.475 (1972).

(16) H. Uchida, F. Kaminaga et al., 10th Japan Heat Transfer Symposium, p.101 (1973).

(17) F. Kaminaga, Ph. D. Thesis, Dept. of Engr. University of Tokyo, Tokyo, 1976.

(18) S. Aoki et al., Annual Meeting of Atomic Energy society of Japan. November, 1974.